Title

CHEMISTRY AND MORPHOLOGY OF COAL LIQUEFACTION ANNUAL REPORT - OCT. 1, 1982 - SEPT. 30, 1983.

Author

Heineinann, H.

Publication Date

1983-09-01

LBL-16773
UC-90d

Lawrence Berkeley Laboratory
UNIVERSITY OF CALIFORNIA

Materials & Molecular Research Division

CHEMISTRY AND MORPHOLOGY OF COAL LIQUEFACTION
ANNUAL REPORT - October 1, 1982 - September 30, 1983

H. Heinemann

September 1983

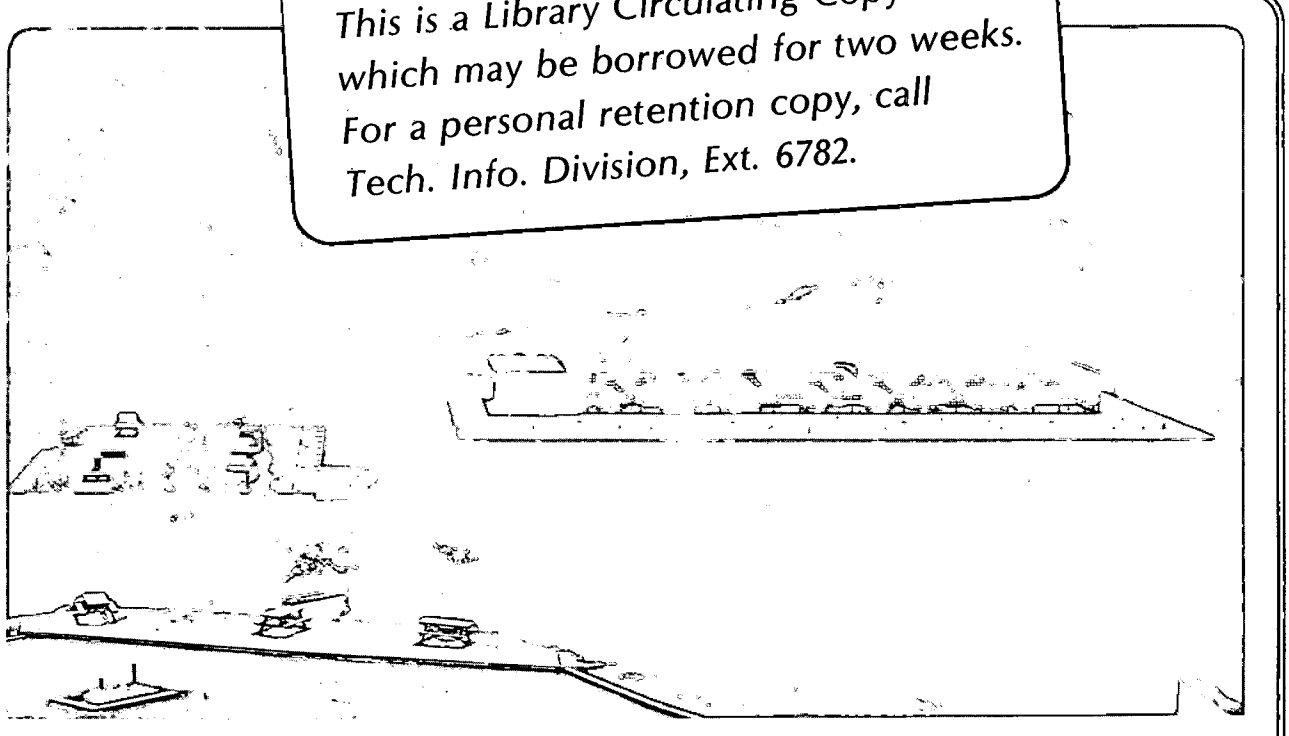

Prepared for the U.S. Department of Energy under Contract DE-AC03-76SF00098

DISCLAIMER

ANNUAL REPORT

October 1, 1982 - September 30, 1983

CHEMISTRY AND MORPHOLOGY OF COAL LIQUEFACTION

Contract ET-78G-01-3425
4006 / 4048

Principal Investigator: Heinz Heinemann

Lawrence Berkeley Laboratory

University of California

Berkeley, California 94720

This work was jointly supported by the Director, Office of Energy Research, Office of Basic Energy Sciences, Chemical Sciences Division and the Assistant Secretary for Fossil Energy, Office of Coal Research, Liquefaction Divison of the U. S. Department of Energy under Contract DE-AC03-76SF00098 through the Pittsburgh Energy Technology Center, Pittsburgh, PA.

CONTENTS

I. Introduction

Because of the funding cuts for Fiscal Year 1983 by Fossil Energy, Liquefaction Division of the Office of Coal Research, U. S Department of Energy, Tasks 2, 4, and 6 were discontinued. The present report covers progress in Tasks 1, 3, and 5.

II. Technical Program for Fiscal 1983

Task 1: SELECTIVE SYNTHESIS OF GASOLINE-RANGE COMPONENTS FROM SYNTHESIS GAS
A. T. Bell

The kinetics for the synthesis of hydrocarbons will be investigated in a well-stirred slurry reactor as well as in a fixed bed reactor. A comparison will be made for product distributions obtained with a series of supported iron catalysts on different support materials. The degree to which the formation of high molecular weight products can be curtailed will be examined as a function of support pore size and composition as well as of reaction conditions.

Task 3: CATALYZED LOW TEMPERATURE HYDROGENATION COAL
G. A. Somorjai

The mechanism of the formation of hydrocarbons from graphite, char, or coke by the reaction with water in the presence of alkali or earth alkali catalysts will be further investigated. The recent finding that C_2 and C_3 hydrocarbons can be formed at low temperatures deserves close scrutiny. The ultimate objective will be to show that the reactions proceeding in a coal gasifier and in a synthesis unit can be combined in a single reactor.

Task 5: CHEMISTRY OF COAL SOLUBILIZATION AND LIQUEFACTION
R. H. Fish and T. Vermeulen

Mechanisms of the selective hydrogenation of nitrogen-containing polynuclear aromatic hydrocarbons by means of ruthenium and rhodium carbonyl phosphine catalysts will be investigated. Questions concerning catalyst stability and catalyst poisoning will be resolved. The ultimate aim is to provide the leads for a

process of hydrogenative removal of nitrogen without saturating all rings of a polynuclear aromatic and thereby saving about 75% of hydrogen consumption.

III. Highlights

Task 1: SELECTIVE SYNTHESIS OF GASOLINE RANGE COMPONENTS FROM SYNTHESIS GAS
A. T. Bell, Project Manager

1) Kinetics of Fischer-Tropsch synthesis over a potassium promoted fused iron catalyst were studied as a function of catalyst reduction conditions. Severe reduction leads to a very active catalyst, which deactivates rapidly. Milder reduction conditions give a less active but more stable catalyst. Differences in the order of dependence on H_2 and on CO and the fact that activation energies are independent of reduction condition suggest that different fractions of the surface are brought into an active state.

2) A study of potential support-metal interaction was undertaken. There are significant differences in the product spectrum between fused Fe_2O_3 and precipated Fe_2O_3 catalysts. Supported iron on silica, mordenite, y-zeolite and ZSM-5 indicated that chain growth probability is the same for all these supports. Olefin to paraffin ratio increases with increasing Al/Si ratio. Dependencies of rates of formation of individual products on H_2 and CO partial pressure are different for each support.

Task 3: CATALYZED LOW TEMPERATURE HYDROGENATION OF COAL
G. A. Somorjai, Project Manager

1) Powdered graphite samples loaded with various amounts of KOH have been reacted with atmospheric pressure of steam in the temperature range 700 - 900K. C_{1-6} hydrocarbons are found in the gaseous products of this reaction. The direct production of C_{2+} hydrocarbons from steam and carbon is a novel finding. Both the abundance of these hydrocarbons with respect to hydrogen and their relative distribution varies as a function of reaction time, KOH loading and temperature. A model for their production is proposed according to which C-H groups are stabilized by the formation of a potassium phenolate type compound at the prismatic edge of graphite.

Hydrocarbons would then be produced from the direct hydrogenation of surface carbon atoms. The hydrocarbon distribution shows large deviations from the ideal Schulz-Flory distribution, giving little support to a chain growth type mechanism.

2) The reaction of KOH loaded graphite powder with atmospheric pressure of steam in the temperature range 700 - 900K proceeds via two successive stages. During Stage I, hydrogen and hydrocarbons are evolved at a high rate but no CO or CO_2. This stage ceases after the equivalent of 0.5 molecules of H_2 per potassium in the sample are produced. During Stage II gasification proceeds catalytically at a much reduced rate with the production of one CO molecule per equivalent H_2 molecule. The absence of CO or CO_2 evolution during Stage I indicates the formation of a stable oxygen containing compound. This compound may be decomposed thermally by heating the sample up to 1300K. CO evolves almost exclusively during this high temperature treatment. These results suggest a step reaction mechanism involving: (1) the dissociative adsorption of water forming C-H and C-OH (phenol) groups, (2) the formation of a K-O-C entity (phenolate), from the reaction of KOH with the phenol groups, (3) the decomposition of these K-O-C entities to give CO, K_2O and perhaps metallic potassium, and (4) the formation of KOH from reaction of K_2O with water. The transition from Stage I to Stage II is due to the consumption of KOH to form K-O-C species. The rate of the catalytic reaction (Stage II) is controlled by the slowest step (3).

3) While the results described in (2) indicate a stoichiometric reaction, recent work with an Illinois #5 char shows that hydrocarbon production does not stop when all potassium hydroxide has been converted as in the case of graphite. It appears that a component in the ash catalytically decomposes the phenolate at reaction temperature, reconstitutes the potassium hydroxide and permits a continuous hydrocarbon production.

Task 5: CHEMISTRY OF COAL SOLUBILIZATION - HOMOGENEOUS CATALYTIC HYDROGENATION REACTIONS OF MODEL FUEL COMPOUNDS
R. H. Fish, Project Manager

1) Deuterium experiments with quinoline, phenanthridine and 7,8-benzoquinoline provide evidence for reversibility in the hydrogenation of the carbon-nitrogen double bond, stereoselectivity in the reduction of the 3,4-double bond (quinoline and 7,8-benzoquinoline), and exchange (cyclometallation) of the aromatic carbon-hydrogens beta (quinoline, phenanthridine) and gamma (7,8-benzoquinoline) to the nitrogen atom.

2) Steric and electronic effects are important in competitive binding experiments designed to find model coal constituents that inhibit and enhance the rate of hydrogenation of quinoline.

3) $(\emptyset_3P)_3RuHCl$ is a better catalyst (faster rates) than its rhodium equivalent, $(\emptyset_3P)_3RhCl$.

4) Polymer-supported Wilkinson's Catalyst hydrogenates the model coal compounds studied at rates that are 10-20 times faster than the homogeneous analog.

5) Catalytic transfer (metal catalyzed) of hydrogen from 9,10-dihydrophenanthridine, 1,2-dihydroquinoline and 9,10-dihydroacridine to other nitrogen heterocyclic compounds provides information on the plausible mechanisms for similar occurences in donor-solvent coal liquefaction processes.

IV. Summary of Studies

Task 1: SELECTIVE SYNTHESIS OF GASOLINE-RANGE COMPONENTS FROM SYNTHESIS GAS
A. T. Bell, Project Manager

Two sets of investigations have been conducted during the past year. One was aimed at establishing the effects of catalyst pretreatment and reaction condi-

tions on the kinetics of Fischer-Tropsch synthesis in a slurry reactor. The objective of the second investigation was to determine the effects of catalyst preparation and the influence of metal-support interactions on the synthesis of hydrocarbons over supported and unsupported Fe.

The kinetics of Fischer-Tropsch synthesis over a fused iron catalyst, promoted with potassium, have been investigated in a well-stirred slurry reactor. Catalyst activity and stability was found to be a strong function of the pretreatment used. Reduction at 300°C for extended time (2 to 3 days) produced a very active catalyst but one that deactivated rapidly, presumably due to the formation of free carbon. As the time and temperature of the catalyst reduction are reduced the catalyst becomes more stable but less active. The kinetics of hydrocarbon synthesis are also sensitive to pretreatment conditions. Following severe reduction, the synthesis rate law exhibits a 0.8 to 1.0 order dependence on H_2 and zero-order dependence on CO. Milder reduction conditions increase the H_2 independence from 1.0 to 1.24 and the CO dependence from 0.2 to 0.4. Interestingly though, the activation energies are unaffected by reduction conditions and typically are between 23 and 27 kcal/mol. These observations suggest that changes in the catalyst activity resulting from differences in reduction conditions, are due primarily to changes in the fraction of the total catalyst surface brought into an active state, rather than being caused by major changes in the synthesis kinetics.

To explore further the influence of catalyst composition on catalyst activity and selectivity, experiments were conducted with Fe_2O_3 and Fe_2O_3 promoted with potassium. The product spectrum over Fe_2O_3 is significantly different from that observed over fused iron. The ratio of β-to α-olefins is significantly higher for synthesis over Fe_2O_3 but the proportion of branched hydrocarbons is significantly less. Secondary hydrogenation also appears to occur more rapidly over Fe_2O_3 than over fused iron. This is evidenced by lower olefin to paraffin ratios and high yields of alcohols relative to aldehydes.

The products produced over a potassium-promoted Fe_2O_3 catalyst are nearly identical to those formed over the fused iron catalyst (which is also potassium-promoted). The presence of potassium appears to enhance the degree of hydrocar-

bon branching, and to decrease the hydrogenation of olefins and aldehydes. Samples of the used catalyst are currently being analyzed by x-ray diffraction to determine the bulk composition of the catalyst, so that it can be compared with that of the used fused-iron catalyst.

The properties of various supported and unsupported iron catalysts were studied using a fixed bed reactor. Fused iron and precipitated iron catalysts produced similar product distributions. The latter catalyst was more active, but only because of its higher surface area. More recently, comparison has been made of Fe/SiO_2, Fe/Mord., Fe/Y-Zeol., and Fe/ZSM-5. The results show the following features:

1. The probability of chain growth, α, is essentially the same on all four supports and at temperatures below 300°C. There is no evidence for cutoff in chain growth. These results suggest that neither the acidity nor the pore structure of the support influences the chain growth and termination processes.

2. All four catalysts produce β-olefins in quantities comparable to α-olefins, and the ratio of β to α-olefins is greater than that observed over fused iron catalysts.

3. The olefin to paraffin ratio increases with increasing Al/Si ratio of the support.

4. The apparent activation energies for paraffin synthesis are greater than those for olefin synthesis, for Fe/SiO_2 and for Fe/Y-Zeol. For Fe/Mord., the apparent activation energies for olefins and paraffins are comparable.

5. The dependencies of the rates of formation of individual products on H_2 and CO partial pressures are different on each catalyst. There appears to be no definite trend in the power law dependencies with the Al/Si ratio of the support, or with support acidity.

6. Little evidence of aromatic products was observed over any of the catalysts for temperatures below 300°C. Above 300°C (up to 320°C) all four catalysts produced aromatics to a comparable degree, suggesting that support acidity is very likely not necessary for the formation of aromatic products.

Task 3: CATALYZED LOW TEMPERATURE HYDROGENATION OF COAL
G. A. Somorjai, Task Manager

The extensive work performed on this task during fiscal 1983 is described in two LBL reports which are appended to this report and which have been accepted for publication in "Applied Catalysis", resp. "Carbon".

Work in progress at report time indicates that the stoichiometric limitation imposed by formation of a potassium phenolate can be overcome and the reaction which produces C_{1-6} hydrocarbons can be made catalytic. Use of an Illinois #5 char, impregnated with KOH resulted in a continuous production of H_2, hydrocarbons and CO. A component of the ash, probably pyrite, appears to decompose the phenolate or inhibit its formation. It is of interest that the C_{2-6} hydrocarbons formed are largely olefinic. While the total amount of such hydrocarbons is at present relatively small, attempts will be made in 1984 to increase them as well as to identify catalysts promoting their formation.

Task 5: CHEMISTRY OF COAL SOLUBILIZATION - HOMOGENEOUS CATALYTIC HYDROGENATION REACTIONS OF MODEL FUEL COMPOUNDS
R. H. Fish, Project Manager

1) <u>The Role of Wilkinson's Catalyst in the Hydrogenation of Quinoline</u>

In order to understand the mechanism of hydrogenation of quinoline with Wilkinson's Catalyst, $(\emptyset_3P)_3$ RhCl, we substituted deuterium gas (D_2) for hydrogen (H_2) and analyzed the product, 1,2,3,4-tetrahydroquinoline, by both 400MHz ^1H NMR spectroscopy and by GC-MS.

Equation 1 describes the results from both above-mentioned techniques. The re-

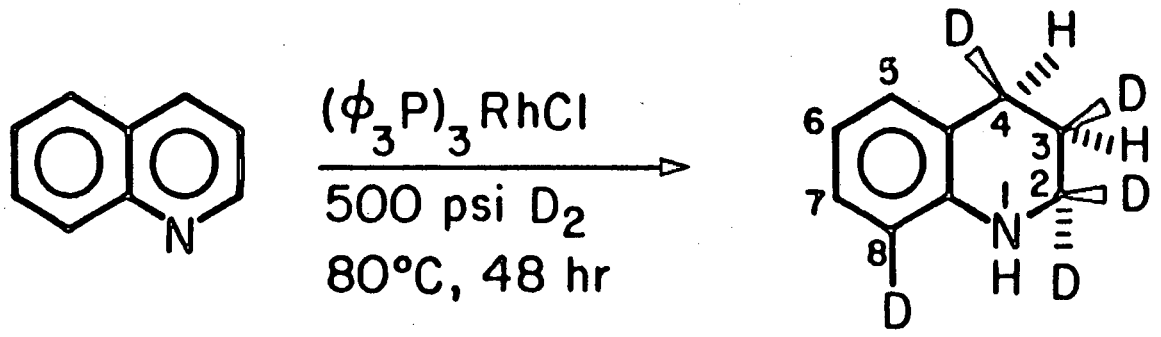

(1)

I 2

GCMS shows D_3 to D_5 for compound 2

NMR shows: ~1.6 D at Position 2
~1.0 D at Position 3
~1.0 D at Position 4
~0.7 D at Position 8

EQUATION 1

400 MHz ^1H nmr shows hydrogens on carbons 3 and 4 to be *cis* to each other.

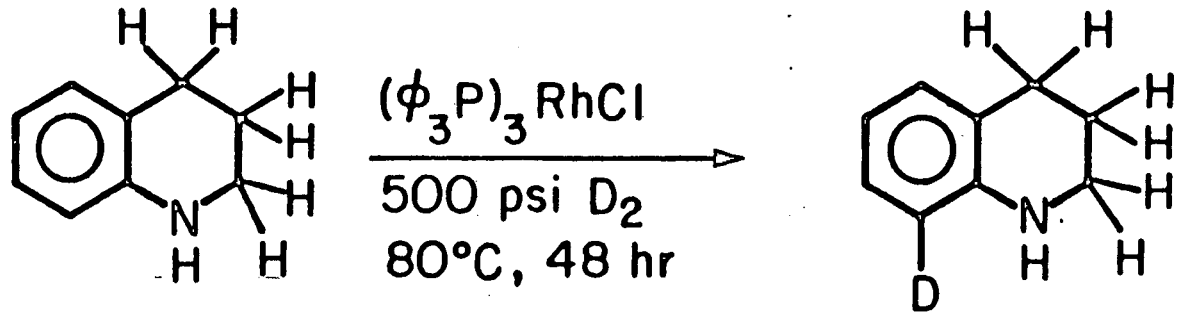

(2)

sults are as follows: a) more-than-one deuterium (1.60) is incorporated in the 2 position; b) stereochemistry for the reduction of the 3,4 double bond is CiS; and c) exchange of the 8 position hydrogen for deuterium implicates cyclometallation reactions and dehydrogenation of the NH-CH_2 grouping on positions 1 and 2 via the incorporation of two deuteriums at carbon 2. Interestingly, the product, 1,2,3,4-tetrahydroquinoline, exchanges only the 8 position hydrogen for deuterium under similar conditions used in the D_2 experiments with quinoline (Eq2).

EQUATION 2

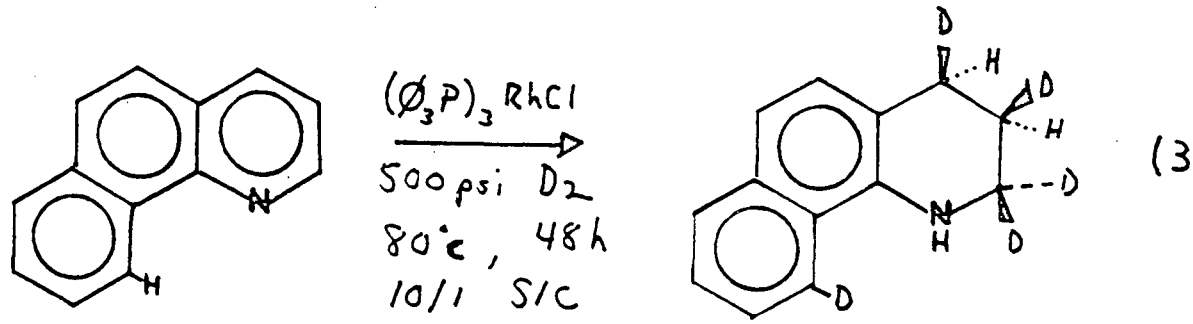

We also discovered recently that a trace of quinoline remaining in the deuteration reaction had a mass spectrum that showed a monodeuterated quinoline-d_1. To ascertain the position of deuteration, we repeated the deuterium gas experiment and stopped the reaction at approximately 50% conversion to deuterated 1,2,3,4-tetrahydroquinoline. Analysis of the remaining quinoline by 250MHz ^1H NMR spectroscopy clearly showed quinoline-2-d_1, i.e. deuterium, at the 2 position. Its relative abundance, m/e 130, was 10% compared to the m/e 130 (100%) when the reaction was allowed to go to greater than 98% completion, strongly suggesting that the second deuterium on carbon 2 of the product comes from the build-up of quinoline-d_1 in the reaction mixture. This hypothesis is also strengthened by the deuterium content of the deuterated 1,2,3,4-tetrahydroquinoline formed in the incomplete reaction (approx. 50%). The mass spectrum and 250MHz ^1H NMR spectrum shows only one deuterium in the 2 position.

These results in the deuterium gas experiments allows the reactions shown in Equation 3 to occur in the complex hydrogenation of quinoline.

EQUATION 3

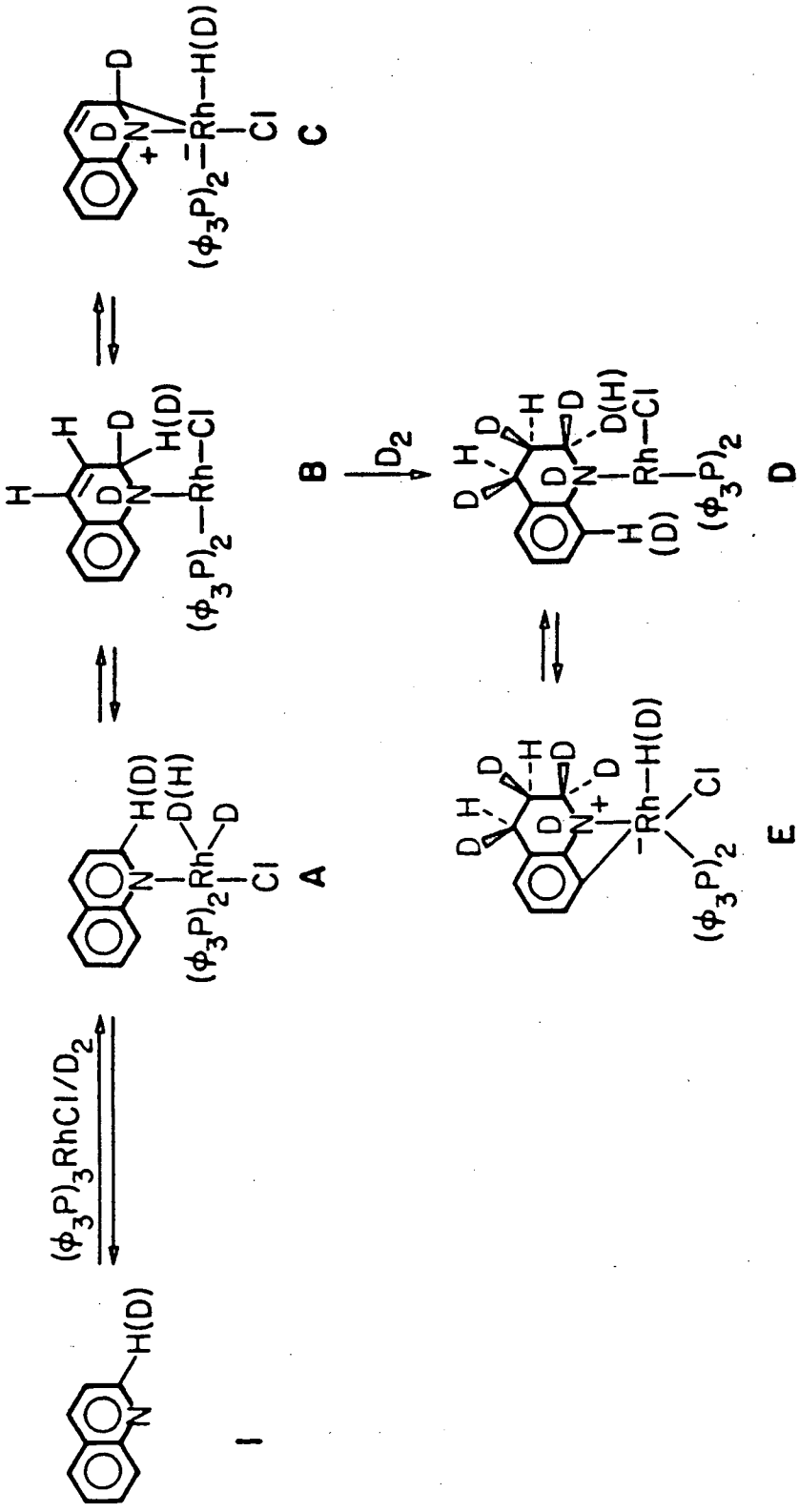

2) Deuterium Gas Experiments with 7,8-Benzoquinoline

In the previous section (1), we described the results of a deuterium gas experiment with quinoline. We have extended these results to the reduction of 7,8-benzoquinoline with D_2 gas, providing a compound that has four deuterium (GC-MS) incorporated, i.e., 1,2,3,4-tetrahydro-7,8-benzoquinoline-d_4. We used 250MHz ^{1}H NMR spectroscopy to ascertain the position of deuterium incorporation. Equation 3 depicts the deuterium pattern and it is entirely similar to that we found in the quinoline reduction with D_2 gas and $(\emptyset_3P)_3RhCl$ as the catalyst. Thus, we found approximately 1.5 D at position 2 and 1.0 D each at carbons 3 and 4 and are in the process of obtaining a 400MHz ^{1}H NMR spectrum to determine the stereochemistry at those latter positions. As in the quinoline reduction, we also observed aromatic hydrogen exchange. The exact position on the aromatic ring has not been accurately determined by 400MHz ^{1}H NMR spectroscopy; however, we postulate that H-9 is the site of exchange (0.5 D) by analogy to previous reports on the metal complexes of phenanthridine. These metal complexes show structures with the metal coordinated to the nitrogen atom and a cyclometallaton at H-9, i.e., insertion of the metal at the C-H bond on carbon 9.

3) Inhibition Studies in the Hydrogenation of Quinoline

Studies on the types of fuel compounds which can potentially inhibit the hydrogenation of polynuclear heteroaromatic nitrogen compounds has continued this year. We were able to use graphing programs with our Apple II computer system to illustrate this inhibition or enhancement of rate with quinoline as the model polynuclear nitrogen heteroaromatic. Figure 1 shows that: 1) pyridine totally inhibits the hydrogenation of quinoline; 2) thiophene has no effect; 3) at 50% conversion, the product, 1,2,3,4-tetrahydroquinoline retards the rate; and 4) indole, which is not reduced itself, enhances the rate of reduction of quinoline. These results are summarized in Chart 1.

Thus, basicity seems to dominate the inhibition of quinoline hydrogenation, while those less basic constituents like thiophene either have no effect or as in the case of indole, enhance hydrogenation using $(\emptyset_3P)_3RhCl$ as the catalyst.

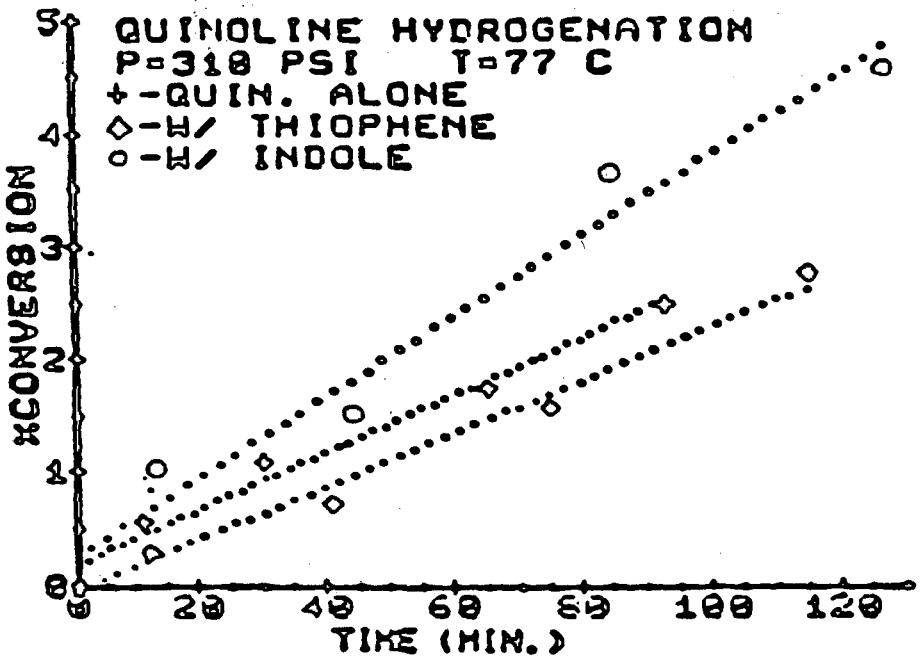

DATA:

PRES.	COMPOUND	RATE
310 (PSI)	PYRIDINE	0.0 (%/HR)
" "	THIOPHENE	1.4
" "	1,2,3,4-THQ	0.6
" "	INDOLE (1)	2.0
" "	INDOLE (2)	2.1

Figure 1

Quinoline Hydrogenation Inhibition Studies/Rate Studies

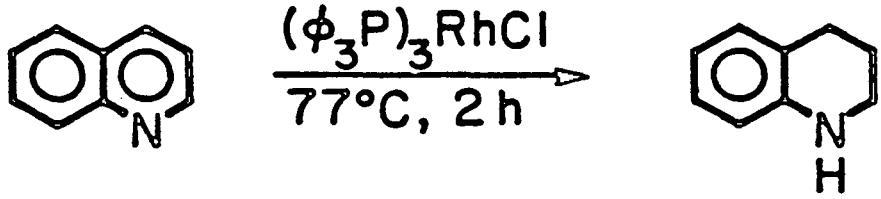

inhibits reduction, but is not reduced itself.

does not inhibit reduction and is not reduced.

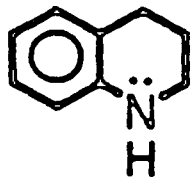

retards rate of reduction by a factor of 0.4.

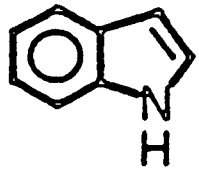

increases rate of reduction by a factor of 1.3, but is not reduced itself.

CHART 1

In several experiments to determine the significance of steric and electronic effect in the inhibition rates of the hydrogenation of quinoline we studied two substituted pyridines, i.e., 2 and 3-methylpyridine. Both these methyl-substituted pyridines have pkb's lower than pyridine itself; thus they are stronger bases.

As with pyridine, 3-methylpyridine completely inhibited the rate of hydrogenation of quinoline, while 2-methylpyridine only inhibited the rate by 43%, i.e., .07% conversion/min. (alone) versus .045%/min. (2-methylpyridine). Clearly, steric (2-methylpyridine) and electronic effects are important parameters in the competitive binding of substrates that can inhibit the rate of hydrogenation of model coal compounds.

4) Competition Studies in the Selective Hydrogenation of Polynuclear Heteroaromatic Nitrogen Compounds

We wanted to determine the relative rates of hydrogenation of polynuclear heteroaromatic nitrogen compounds that have previously been studied as model synthetic fuel compounds in homogeneous hydrogenation reactions. These relative rates are important for future studies on the reductions of mixtures of these compounds. Table 1 provides the results and indicates with both $(\emptyset_3P)_3RuHCl$ and $(\emptyset_3P)_3RhCl$ that competitive inhibition and, in the rhodium case, enhancement occurs with added model coal constituents. In fact, the $(\emptyset_3P)_3RuHCl$ is a better catalyst (i.e., faster rates) but is not affected by compounds that enhance the rate of quinoline hydrogenation compared to Wilkinson's Catalyst.

Such data will be important in practical applications using these catalysts.

5) Hydrogen Transfer Versus Hydrogenation Catalysts

We have discovered that certain saturated nitrogen heterocyclic model coal compounds can be hydrogen donors in catalytic hydrogen transfer reactions. The relevance to a coal liquefaction process comes from attempting to understand the role of metal compounds in donor-solvent coal liquefaction processes, which is an area that has not been studied to any significant extent on a basic level.

Table 1: Comparison of $(\phi_3P)_3RuHCl$ and $(\phi_3P)_3RhCl$ in Individual and Competitive Hydrogenation Studies

INDIVIDUAL RATES*

Substrate	$HRu(PPh_3)_3Cl$		$Rh(PPh_3)_3Cl$		Act. Rate(Ru)/ Act. Rate (Rh)
	Act. Rate (%/min.)	Rel. Rate	Act. Rate (%/min.)	Rel. Rate	
Quinoline	0.47	1.00	0.079	1.00	5.9
5,6-Benzoquinoline	0.059	0.12	0.03	0.38	2.0
7,8-Benzoquinoline	0.014	0.03	0.013	0.16	1.1
Acridine	4.3	9.15	0.21 (0.12)**	2.7 (1.5)**	20
Phenanthridine	11 (approx.)	24 (approx.)	6 (approx.)	76 (approx.)	1.8 (approx.)
Indole	0.085	0.18	0.00	0.00	---
Benzothiophene	0.041	0.09	0.12	1.52	0.34

*10.1 Substrate/Catalyst Ratio, 310 psi H_2 (initially), 85°C.
**Rate in parenthesis is conversion to the tetrahydroproduct.

COMPETITION STUDIES WITH QUINOLINE***

Substrate	$HRu(PPh_3)_3Cl$				$Rh(PPh_3)_3Cl$			
	Act. Quin. Rate	Rel. Quin. Rate	Act. Sub. Rate	Rel. Sub. Rate	Act. Quin. Rate	Rel. Quin. Rate	Act. Sub. Rate	Rel. Sub. Rate
5,6-Benzoquinoline	0.37	0.79	0.033	0.56	0.073	0.9	0.01	0.33
7,8-Benzoquinoline	0.46	0.98	0.011	0.80	0.095	1.2	0.003	0.25
1,2,3,4-Tetrahydro-quinoline	0.16	0.34	-----	----	0.039	0.5	-----	----
2-Methylpyridine	0.40	0.85	-----	----	0.047	0.6	-----	----
3-methylpyridine	0.00	0.00	-----	----	0.004	0.05	-----	----
Pyrrole					0.12	1.5	-----	----
Indole	0.31	0.66	0.038	0.45	0.15	1.9	-----	----
Carbazole	0.42	0.89	-----	----	0.15	1.9	-----	----
Benzothiophene	0.47	1.00	0.011	0.27	0.15	1.9	0.04	0.33

***1:1 Quinoline/Substrate Ratio, 10:1 Quinoline/Catalyst Ratio, 310 psi H_2 (initially), 85°

We have found that $RuCl_2(\emptyset_3P)_3$ is a very active dehydrogenation catalyst, for example, in the transfer of hydrogen from 9,10-dihydrophenanthridine to quinoline. In that experiment, dehydrogenation of 9,10-dihydrophenanthridine to phenanthridine was very rapid in the presence of $RuCl_2(\emptyset_3P)_3$. In addition, we tentatively found that hydrogen gas (mass spectral studies solidify this point) was the product of the dehydrogenation and that an indirect transfer of hydrogen occurred rather than a direct transfer. Thus, excellent hydrogenation catalysts like $(\emptyset_3P)_3RhCl$ would probably be better catalysts in these transfer reactions.

We recently tested this hypothesis by comparing the rates of hydrogenation of quinoline with both $(\emptyset_3P)_3RuCl_2$ and $(\emptyset_3P)_3RhCl$. Figure 2 dramatically shows that the ruthenium catalyst hydrogenates quinoline six times faster than the rhodium catalyst. Thus what we learned from this one experiment is that catalysts that are efficient in dehydrogenation reactions can also be effective hydrogenation catalysts.

This finding could have important economic effects on the use of these catalysts in practical applications, since ruthenium is economically more viable than rhodium.

6) Relative Rates of Hydrogenation of Polynuclear Heteroaromatics with the Polymer-Supported Wilkinson's Catalyst: A Comparison to the Homogeneous Wilkinson's Catalyst.

In order to compare the homogeneous Wilkinson's Catalyst with its polymer-supported analog under hydrogenation conditions, we have used our kinetic apparatus to obtain the initial rates and relative rates (quinoline = 1.0) of several polynuclear heteroaromatic compounds. Table 2 contains the data and dramatically shows that the rate of hydrogenation of our polynuclear heteroaromatic model compounds are 10 to 20 times faster with the polymer-supported Wilkinson's Catalyst than with the homogeneous catalyst. This is an important result which we don't totally understand. However, it does emphasize the potential of these heterogenized catalysts in practical applications.

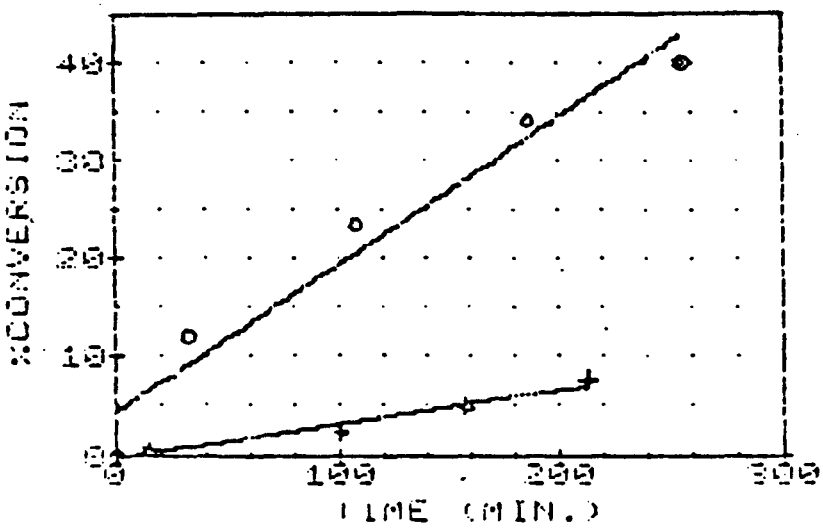

O $(Ø_3P)_3RuCl_2$

\+ $(Ø_3P)_3RhCl$

Conditions: 75°C, 310 psi H_2
substrate/catalyst = 10
in benzene for 4 hr

Figure 2: Rate of hydrogenation of quinoline with $(Ø_3P)_3RhCl$ and $(Ø_3P)_3RuCl_2$ as catalysts.

Table 2: Comparison of Relative Rates for Both Homogeneous and Polymer-Supported Wilkinson's Catalyst in the Selective Reductions of Polynuclear Heteroaromatic Compounds

Substrate[a]	Polymer-Supported Rate[b]	Rel. Rate[c]	Homogeneous Rate[d]	Rel. Rate	Polymer-Supported/ Homogeneous Rate
Quinoline	0.29	1.0	.013	1	22
5,6-Benzoquinoline	0.14	0.48	.007	0.5	22
7,8-Benzoquinoline	0.024	0.08	.001	.09	20
Acridine	0.4	1.4	.037 (approx.)	3.0 (approx.)	11
Benzothiophene	0.029 (approx.)	0.1 (approx.)	0.04	3.4	0.7 (approx.)

a 310 psi H_2; 85°C; 2% cross-linked; 2.2% Rh; substrate to catalyst ratio, 90:1

b %/minute

c relative to quinoline (1.0)

d 310 psi H_2; 5°C; substrate to catalyst ratio 90:1

Conclusions

The potential use of polymer-supported catalysts for the hydroprocessing of coal liquids and shale oil needs to be ascertained; however, our initial results on the low temperature and low pressure hydrogenation of model coal liquids using these catalysts have given important insights into these possibilities and have encouraged us to pursue experiments that will further elucidate these practical applications.

Catalytic transfer hydrogenation has not been studied with regards to donor-solvent chemistry. In addition, the fact that saturated nitrogen heterocyclic compounds (known to form in hydrogenation processes of coal) are excellent sources of hydrogen gas, allows further study of these compounds in transfer experiments with other model compounds such as olefins, etc.

Publications

(1) R. H. Fish, A. D. Thormodsen, and G. A. Cremer
J. Am. Chem. Soc. 104 5234 (1982)

(2) R. H. Fish and A. D. Thormodsen
Selective Reductions of Polynuclear Heteroaromatic Compounds Catalyzed By Chloro (Tristriphenylphosphine) Rhodium (1).
J. Am. Chem. Soc., 1983 (submitted for publication).

(3) R. H. Fish
Selective Reductions of Polynuclear Aromatic and Heteroaromatic Compounds Catalyzed by Transition-Metal Carbonyl Hydrides.
Ann. N. Y. Acad. Sc. 1983 (in press).

V. Future Research Plans

Task 1

It is planned to complete the objectives of the present project during FY 1984. The experimental results obtained for Fischer-Tropsch synthesis over α-Fe, Fe_2O_3, and Fe_3C will be compared to establish patterns in catalytic activity and selectivity as a function of catalyst composition. X-ray diffraction patterns will be taken of the fresh and spent catalysts to determine whether bulk composition changes with time on stream. In particular it would be desirable to know whether these materials achieve a common bulk composition, catalytic activity, and selectivity, after extended use.

Efforts will also be made to interpret the rate data obtained for α-Fe, Fe_2O_3, and Fe_3C in the light of mechanistic models of the reaction kinetics.

The work on supported Fe catalyts will be concluded by obtaining data on the performance of Fe/Al_2O_3, Fe/TiO_2, and Fe/MgO for comparison with the data already available for Fe/SiO_2 and zeolite-supported Fe. All catalysts will be examined in both a calcined and a reduced state to determine the influence of pretreatment. Additional work will also be done with Fe/ZSM-5 to understand better why the zeolite appears to influence the product distribution so little at temperatures below 300°C. It is conceivable that for the zeolite to have an effect, the temperatures must exceed 300°C by a substantial margin.

Task 3

Leads to make the production of higher hydrocarbons from carbon and water truly catalytic will be pursued. It appears possible to catalytically decompose phenolates formed, preventing stoichiometric limitations.

Attempts will be made to greatly increase rates and volume of hydrocarbon formation. This may be accomplished by operation at higher water partial pressure and by catalytic promoters. Further, the addition of CO, resp. Co_2, to the reaction offers indications of producing liquid hydrocarbons.

Task 5

The FY84 program will concentrate on the use of polymer-supported catalysts and their mechanistic implications in the selective catalytic hydrogenation of model coal compounds. This will include experiments with deuterium rates, and competitive reaction to better define potential catalyst poisoning as well as enhancement of rates of selected model coal compounds.

Catalytic cracking of partially hydrogenated nitrogen containing ring compounds will be investigated to determine the total savings of hydrogen in nitrogen removal over conventional hydrocracking.

In addition, we will attempt to define the important parameters in the catalytic transfer of hydrogen from saturated nitrogen heterocyclic compounds to other coal liquid constituents. This will include scope, rates and a perusal of polymer-supported catalysts capable of dehydrogenation-hydrogenation reactions.

The Role of KOH in the Low Temperature Steam Gasification of Graphite: Identification of the Reaction Steps

By F. Delannay*, W.T. Tysoe, H. Heinemann and G.A. Somorjai

Materials and Molecular Research Division, Lawrence Berkeley Laboratory,
and
Department of Chemistry, University of California, Berkeley, CA 94720

Abstract

The reaction of a KOH loaded graphite powder with atmospheric pressure of steam in the temperature range 700-900K proceeds via two successive stages. During stage I, hydrogen and hydrocarbons are evolved at a high rate but no CO or CO_2. This stage ceases after the equivalent of 0.5 molecules of H_2 per potassium in the sample are produced. During stage II gasification proceeds catalytically at a much reduced rate with the production of one CO molecule per equivalent H_2 molecule. The absence of CO or CO_2 evolution during stage I indicates the formation of a stable oxygen containing compound. This compound may be decomposed thermally by heating the sample up to 1300K. CO evolves almost exclusively during this high temperature treatment. These results suggest a step reaction mechanism involving (1) the dissociative adsorption of water forming C-H and C-OH (phenol) groups, (2) the formation of a K-O-C entity (phenolate), from the reaction of KOH with the phenol groups, (3) the decomposition of these K-O-C entities to give CO, K_2O and perhaps metallic potassium and (4) the formation of KOH from reaction of K_2O with water. The transition from stage I to stage II is due to the consumption of KOH to form K-O-C species. The rate of the catalytic reaction (stage II) is controlled by the slowest step (3).

*On leave from the Groupe de Physico-Chimie Minérale et de Catalyse, Université Catholique de Louvain, Belgium

1. INTRODUCTION

Steam gasification of carbon to produce hydrogen and carbon monoxide is usually conducted at a temperature higher than 1000K. The need for such high a temperature is a consequence of the highly endothermic nature of the reaction.

$$C + H_2O \longrightarrow H_2 + CO \qquad (1)$$
$$\Delta H_{300K} = + 31.4 \text{ kcal/mole}$$

Hydrocarbons can subsequently be synthesized from H_2 and CO by methanation or Fischer-Tropsch reactions on suitable catalysts. These reactions are exothermic and are carried out at relatively low temperatures (500–800K).

The direct production of methane according to the reaction

$$2C + 2H_2O \longrightarrow CH_4 + CO_2 \qquad (2)$$
$$\Delta H_{300K} = 3.65 \text{ kcal/mole}$$

is virtually thermoneutral. This has prompted the search for catalysts able to activate this reaction at low temperature. Low temperature operation is also necessary to avoid decomposition of other hydrocarbons that might be formed.

Alkalis are known to catalyse reaction (1) [1,2,], and the presence of alkali hydroxides has been reported to bring about the formation of methane from the reaction of graphite with water vapor in the temperature range 500–800K[3,4]. These experiments used small pices (~ $1cm^2$) highly oriented pyrolytic graphite (Union Carbide) which was exposed to 20

Torr of water vapor in a recirculation type reactor. At 500K, surface carbon atoms were shown to be converted into CH_4 with an apparent turnover frequency of 1 to $5x10^{-4}$ s^{-1}.

The influence of KOH on the low temperature reaction of carbon with water vapor has now been studied on larger surface area powder graphite samples exposed to atmospheric pressure of steam. It was found that KOH indeed promotes the production of hydrogen, methane and other hydrocarbons at temperatures below 800K but that this reaction is stoichiometric rather than catalytic. The present paper studies the stoichiometric versus catalytic behaviors observed in the temperature range 600-1000K. It is shown that both behaviors can be rationalized within the framework of the same reaction mechanism. A subsequent paper [5] will deal with the influence of experimental conditions on the distribution of the hydrogen and hydrocarbon reaction products.

2. EXPERIMENTAL

The carbon used in these experiments was spectroscopic grade graphite powder (Ultra Carbon Corp., Type UCP-2, 325 mesh) having a BET surface area of 30 m^2g^{-1}. Incipient wetness impregnation was performed by mixing equal weights of graphite powder and of a solution of KOH or K_2CO_3 (Mallinckrodt, analytical grade) in distilled water. The potassium/carbon loading was varied by changing the solution concentration. The sample was then dried at 375K for about 30 minutes.

Figure 1 presents a diagram of the experimental setup. The reactor was a 3.7 mm ID alumina tube in which 0.5 g of sample was deposited

between two alumina wool plugs. Quartz or stainless steel were avoided because, under reaction conditions, these materials were found to react with KOH and/or affect the rate and product distribution of the reaction. The reactor furnace temperature could be adjusted from 300K to 1300K.

The sample could be exposed to either pure argon or pure steam. Steam was produced by pressurizing a distilled water reservoir with argon so as to force water through a heated tube (steamer) where it was vaporized. The steam pressure in the reactor was thus equal to the argon pressure. Usually, a pressure slightly in excess of atmospheric pressure yielded a flow rate of about 50cc of gas min^{-1}. This produced a sufficiently high water vapor space velocity that the reaction was far from equilibrium over the whole temperature range.

At the outlet of the reactor, steam was condensed in an open ended U-shaped tube immersed in water. The gas products which bubbled out of the tube were collected in a 3cc graduated burette filled with water. This allowed a precise measurement of the rate of gas evolution. The whole collecting system contained less than 40 ml of water so as to minimize the possibility of dissolution of the gas products. At the top end of the burette, a septum allowed sampling of the gases for immediate analysis. The products could also be stored in a vacuum container for later analysis after completion of the reaction.

The products were analysed by gas chromatography and mass spectrometry

A thermal conductivity detector with a column consisting of six feet Chromosorb 102 + six feet Chromosorb 101 with argon carrier was used for the analysis of H_2, CO, CO_2, and CH_4. A flame ionization detector with a six feet long Chromosorb 102 column and argon carrier was used for the analysis of the hydrocarbons. Mass spectrometry of the products was performed by leaking the gas stored in the vacuum container into an ultra high vacuum chamber equipped with a EAI quadrupole mass spectrometer [3]. Mass spectrometry was mainly used to assess whether Ar, O_2 or air were present in the products. A small amount of argon was usually found due to solution in the water. In some experiments involving low gas production rates, this amount of argon had to be subtracted in order to determine the volume of gas products accurately.

3. RESULTS

Three types of experiments were conducted: isothermal reactions in the presence of steam; temperature programmed reactions with steam, and temperature programmed heating in an argon atmosphere.

a) Isothermal Reactions

In these experiments, the sample was first exposed to steam at about 400K. The temperature of the reactor was then raised quickly ($\sim$ 160K min^{-1}) up to a reaction temperature in the range 700-900K. Figure 2 shows the amount of gas collected as a function of time at 800K for a sample having a KOH/carbon molecular ratio of 0.043 (corresponding to 20% of KOH by weight). The shape of this plot is typical of all reactions

in this temperature range (700-900K) for KOH/C ratios varying from 0.01 to 0.065. The amount of gas produced has been normalized to the number of KOH molecules in the sample. After an initial burst of gas, a first steady state production was observed for a few hours. During this first steady state, the products were only hydrogen and hydrocarbons with virtually no detectable CO and CO_2. The hydrocarbon/hydrogen molecular ratio during this phase ranges from 0.5×10^{-2} to 5×10^{-2}, the largest hydrocarbon component being methane. However, higher hydrocarbons up to C_6 are easily detectable in the product gas. Their proportions depend on reaction time and temperature and alkali loading.[5]

The reactivity of the sample then decreased usually over a fairly short period. This phenomenon always occurred as soon as the equivalent of 0.5 H_2 molecule per potassium atom in the sample had been collected. The gas production subsequently proceeded with a much reduced rate. CO was found in the products during this second steady state, as indicated by the dashed line in Figure 2. The rates of production of CO and H_2 during this low rate were approximately equal as expected from reaction (1). A few of percent of CO_2 could also be detected.

The first and second steady states exhibited in Figure 2 may for the present be assumed to be due to two different reactions. These reactions will be referred to in the following as reactions I and II respectively.

In order to assess whether reaction I is due to the mere dehydrogenation of KOH, the sample was heated under an argon atmosphere instead of flowing steam. No gas was produced, indicating that water is required for the reaction.

The activation energy of reaction I was measured on samples with a KOH/C ratio of 0.043 (corresponding to a C/KOH ratio of ~23) in the temperature range 850-1000K. The determination was made after the collection of about 0.15 to 0.2 gas molecules per potassium. As shown by the Arrhenius plot of Figure 3, these rates yield an accurate activation energy of 44.8 kcal/mole.

As shown on the semilog plot of Figure 4, the rate of reaction I at 800K (expressed as number of gas molecules per potassium per unit time) increased drastically when increasing the KOH/C ratio from 0.01 to 0.04 (corresponding to a decrease in C/KOH ratio from 100 to 25). No marked change was observed from 0.04 to 0.065.

In order to check whether the behavior of potassium carbonate was identical to that of potassium hydroxide, an isothermal reaction was conducted at 800K on a sample with a K_2CO_3/C molecular ratio of 0.0215 (so that it contains the same number of potassium atoms as an alkali hydroxide loaded sample with KOH/C=0.043). Apart from a burst of gas which corresponds to the formation of about 0.01 gas molecule, per potassium atom, no type I reaction was observed, merely a much slower type II reaction.

b) Temperature Programmed Reaction

In these experiments, the sample was exposed to steam at 500K (ie. before significant reaction had commenced) and the temperature of the reactor was increased at a constant rate of 5K min^{-1}. The open circles in Figure 5 show the resulting rate of gas production as a function of temperature for a sample with a KOH/C ratio of 0.043. A maximum is observed at a temperature of about

900K. The decrease in rate after this maximum reflects the same phenomenon as the transition from reaction I to reaction II in isothermal reactions (Figure 2). The total gas produced at the end of this decrease corresponds again to about 0.5 equivalent hydrogen molecules per potassium. When the temperature is increased further, the reaction rate once again starts to increase exponentially with increasing temperature. This stage of the reaction apparently corresponds to reaction II in isothermal experiments. (Extrapolating this steeply increasing plot down to 800K would yield a rate corresponding approximately to the slope of the plot in region II of Figure 2).

The solid points in Figure 5 are the rates of production for a similar experiment for a sample containing K_2CO_3 instead of KOH (K_2CO_3/C=0.0215). Only the high temperature type II reaction is observed. This rate is however lower than for the KOH loaded sample.

A blank experiment with a sample of pure graphite powder in the absence of KOH exhibited a gas production which was too low to allow an accurate measurement of its temperature dependence. At 1050K, the gas production rate in the absence of alkali was about 40 times lower than for the sample with KOH/C=0.043.

Figure 6 replots the data of Figure 5, in Arrhenius form. In the case of a KOH loaded sample, the rates at temperatures below the maximum (reaction I) do not follow a single straight line.

For reaction above 900K (reaction II), the KOH loaded sample exhibits an apparent activation energy that is 10 kcal/mole lower than that for a K_2CO_3 loaded sample.

c. Temperature Programmed Heating Under Argon

If all the hydrogen produced during reaction I comes from the steam alone, the corresponding amount of oxygen should be accumulated in the sample in the form of an oxygen containing compound. We have attempted to thermally decompose this compound. A sample with a KOH/C ratio of 0.043 was reacted isothermally with steam at 800K up to the completion of reaction I. After flowing argon for about 1 hour at the reaction temperature in order to remove all remaining water, the argon flow was turned off and the sample heated at a linear rate of 15K min^{-1} without gas flow. Gas desorption caused gas to issue from the reactor into the collecting burette, allowing an accurate measurement of the rate of desorption (after correction for the thermal expansion of gas in the reactor). Fig. 7 shows plots of the time dependence of reactor temperature and gas desorption rate. The temperature of the reactor could not be increased above 1300K so that the position of the maximum desorption rate has little kinetic meaning as it merely coincides with the start of the isothermal period. Figure 8 presents an Arrhenius plot of the rate of desorption at the beginning of the temperature treatment (up to the desorption of 10% of the total). This yields an apparent activation energy of 35.4 kcal/mole.

The gas desorbed during this heat treatment was almost exclusively CO, containing only a few percent CO_2. The total CO accumulated after 3 hours

of treatment at 1300K corresponded to a CO/K ratio of about 0.8. A small amount of gas production continued after this period. However, even after overnight heating the total CO/K ratio never reached 1.

No gas was collected during a similar heat treatment of a pure graphite sample.

If the sample was again exposed to steam at low temperature after this heat treatment, it recovered part of its original reactivity. Figure 9 compares the gas production at 800K for a freshly prepared sample and for the same sample after heat treatment and reexposure to atmospheric pressure of steam at 400K. In this case, no linear steady state region was observed, merely a continuous decrease of reaction rate with time. Depending on the duration of the high temperature (1300K) treatment, the amount of hydrogen collected during a 2 hour period corresponded to a H_2/K ratio of 0.08 to 0.15.

4. DISCUSSION

The high gasification rate referred to as reaction I is a specific property of the hydroxide loaded graphite sample. This reaction is evidently not catalytic: water reacts with carbon and potassium hydroxide to produce hydrogen and hydrocarbons whereas oxygen remains in the sample in the form of an unknown oxygenated species. The accumulation of this species eventually results in the deactivation of the sample. As this deactivation always occurs after the production of the same H_2/K ratio, whatever the KOH loading, it appears that this species is associated with potassium in a fixed stoichiometric ratio.

One potential reaction scheme is the conversion of potassium hydroxide into a carbonate according to the equation

$$2KOH + H_2O + C \longrightarrow K_2CO_3 + 2H_2 \qquad (3)$$

This reaction has been proposed in a patent by Shalit et al. [6]. It is only slightly endothermic (ΔG_{800K} = + 11.2 kcal/mole). However, our results do not seem to be in accord with such a reaction since it involves the production of one H_2 per potassium on the sample, whereas only half this amount is evolved. In addition, if KOH had, in fact, been completely converted into K_2CO_3 after completion of reaction I, it should subsequently behave like a K_2CO_3 loaded sample. Figure 6 indicates, however, that the two samples exhibit a 10 kcal/mole difference in apparent activation energy for reaction II.

An alternative reaction scheme is presented in Figure 10. The first step would be the dissociative adsorption of a water molecule on the prismatic planes of graphite to form a phenolic and a C-H group. Such a dissociative adsorption with high sticking probability has been inferred by Olander et al. [7] from molecular beam scattering experiments. In the absence of alkali, these groups rapidly recombine to yield a water molecule once again. A strong base such as KOH would, however, neutralize the weakly acidic phenol group to give a potassium phenolate salt and a water molecule (step 2). In this case, the hydrogen remaining adsorbed on the carbon surface may either desorb as H_2 or sequentially form C-H bonds to yield a hydrocarbon. The ratio of hydrogen to potassium predicted by this reaction scheme (0.5) corresponds to that observed experimentally.

Moreover, the existance of such phenolate groups as intermediates in the catalytic gasification of carbon has been previously postulated by Mims and Pabst [8,9]. It should, however, be noted that, in the present case, the number of potassium atoms in the sample is much larger than the number of accessible edge sites on the graphite surface. Thus it is necessary to assume that the interaction of potassium with the carbon surface induce weakening and, eventually, scission of the C-C bond so as to create new surface sites for reaction. Such a fragmentation of the aromatic rings due to the interaction with potassium has, for example, been suggested by Sancier [10] on the basis of the e.s.r. analysis of a heat treated K_2CO_3-carbon mixture. The chemical nature of the compound containing the K-O-C groups is unknown. It might be suggested that these groups end up as potassium carbonyl entities stabilized by some interaction (eg. intercalation) with graphite.

Heat treatment of the sample after complete conversion of the KOH induces the decomposition of these K-O-C groups to yield, either metallic potassium and CO, or K_2O, CO and carbon (step 3 in Figure 10). Metallic potassium evaporates at a high rate at 1050K, so that much of the metallic potassium could sublime from the sample during heat treatment at 1300K. (Some intercalation might also occur [11]). K_2O remains in the sample and converts into KOH under subsequent exposure to steam so as to restore part of the activity of the sample (step 4). If the ratio m = CO/K collected during heat treatment equals 0.85, 30% of the original KOH loading is then

available for reaction. When the sample is reexposed to steam, the resulting gas production should yield an amount of H_2 corresponding to $H_2/K=0.15$ (with respect to the original KOH loading) which corresponds to that observed experimentally.

It is worth noting that the amounts of gas collected during the first reaction, high temperature treatment and subsequent reaction, all rule out the conversion of KOH into K_2CO_3 during reaction I. This is because the collection of a ratio $CO/K < 1$ would imply the decomposition of K_2CO_3 into K_2O, and, in such a case, the original activity of the sample should be completely restored under reexposure to steam. This did not occur, as shown on Figure 9.

The various stages of reaction may thus be rationalized as follows. The initial burst may correspond to the fast reaction of KOH already in contact with prismatic edges of the graphite. The subsequent steady state (reaction I) is controlled by transport of the remaining KOH to these edges and presumably also by the breaking of the C-C bonds necessary to provide enough reaction sites. According to Figure 3, these phenomena have an activation energy of about 45 kcal/mole. (The slopes of the Arrhenius plots for reaction I reported in Figure 6 cannot be taken as accurate activation energies as, in this experiment, one of the reactant phases (KOH) progressively disappears.)

After completion of reaction I, the gas production is controlled by the decomposition of the K-O-C groups (step 3 in Figure 10). The mechanism of reaction II (which is obviously catalytic) involves the whole set of sequential

steps as proposed in Figure 10, step 3 being the rate limiting one. The apparent activation energy measured on the Arrhenius plot in Figure 8 is probably fairly close to the true activation energy for the decomposition of the K-O-C groups (as less than 10% of these groups have been consumed during this experiment so that their coverage remains constant). It is striking that this value corresponds nicely to the activation energy of reaction II measured in Figure 6.

Several authors [12,13] have proposed that the decomposition of alkali carbonate in the presence of carbon to give metallic alkali and CO was the rate limiting step in the alkali carbonate catalyzed steam gasification of carbon. Our conclusions concerning the role of KOH are similar, except that the oxygen containing intermediate appears not to be K_2CO_3. The activation energy for the KOH catalyzed reaction (reaction II) is 10 kcal/mole lower than in the case of K_2CO_3.

5. CONCLUSION

The high rate of carbon gasification promoted by KOH at temperatures even lower than 800K is a striking phenomenon. As discussed in the subsequent paper [5], significant amounts of hydrocarbons are produced under such reaction conditions. This reaction cannot be sustained in a catalytic way, due to the high stability of the oxygen containing potassium compound (K-O-C) that is formed. If a compound can be found that plays the same role as potassium hydroxide while yielding a less stable oxygen containing intermediate it would allow the attainment of catalytic gasification without requiring high temperature operation.

ACKNOWLEDGEMENTS

This work was jointly supported by the Director, Office of Energy Research, Office of Basic Energy Sciences, Chemical Sciences Division, and the Assistant Secretary for Fossil Energy, Office of Coal Research, Liquefaction Division of the U. S. Department of Energy under Contract Number DE-AC03-76SF00098 through the Pittsburgh Energy Technology Center, Pittsburgh, PA.

We also aknowledge partial support of this research by the Air Products Corp.

REFERENCES

1. Weng-Yang Wen, Catal. Rev. Sci. Eng., 22, 1 (1980).
2. D.W. McKee, in "Chemistry & Physics of Carbon", (P.L. Walker Jr. and P.A. Thrower eds), Vol. 16, pg 1, Marcel Dekker, New York (1981).
3. A.L. Cabrera, H. Heinemann and G.A. Somorjai, J. Catalysis, 75, 7-22 (1982).
4. D.J. Coates, J.W. Evans, A.L. Cabrera, G.A. Somorjai and H. Heinemann, J. Catalysis, 80, 215 (1983).
5. F. Delannay, W.T. Tysoe, H. Heinemann and G.A. Somorjai, submitted to Applied Catalysis.
6. H. Shalit, D. Hill and E.S.J. Tomezsko, U.S. Patent, 3, 786, 138 (1974).
7. D.R. Olander, T.R. Acharya and A.Z. Ullman, J. Chem. Phys., 67, 3549 (1977).
8. C.A. Mims and J.K. Pabst, Am. Chem. Soc. Div. Fuel Chem., Prepr. 25, 258 (1980).
9. C.A. Mims and J.K. Pabst, Fuel, 62, 176 (1983).
10. K.M. Sancier, Preprints Fuel Chem. Div. ACS, 28, 62 (1983).
11. F. Kapteijn, J. Juriaans and J.A. Moulijn, Fuel, 62, 249 (1983).
12. M.J. Veraa and A.T. Bell, Fuel, 57, 194 (1978).
13. D.W. McKee, Carbon, 20, 59 (1982).

FIGURE CAPTIONS

Fig. 1: Diagram of experimental apparatus.

Fig. 2: Plot of gas production as a function of reaction time at 800K for a sample with a KOH/C loading equal to 0.043 (molecular ratio).

Fig. 3: Arrhenius plot of the temperature dependence of gasification rate after the collection of 0.15 to 0.2 gas molecule per potassium in the sample.

Fig. 4: Plot of dependence of the rate of reaction I on the KOH/C loading.

Fig. 5: Plot of the temperature dependence of the gas production rate during a temperature programmed reaction at a heating rate of 5K min^{-1}. The open circles and full dots correspond to KOH and K_2CO_3 loaded samples respectively. The K/C ratio equals 0.043 in both cases.

Fig. 6: Arrhenius plots of the temperature dependence of the gas production rate displayed in Figure 5.

Fig. 7: Plot of the temperature dependence of the CO desorption rate during high temperature treatment of a sample with KOH/C=0.043 after completion of reaction I.

Fig. 8: Arrhenius plot of the temperature dependence of the CO desorption rate at the beginning of the linear heating of a sample during the same experiment as displayed in Figure 7.

Fig. 9: Plot of a comparison of the gas production as a function of time for a freshly prepared KOH loaded sample (a) and for the same sample after high temperature treatment (b).

Fig. 10: Mechanistic model for the reaction of water with graphite in the presence of KOH.

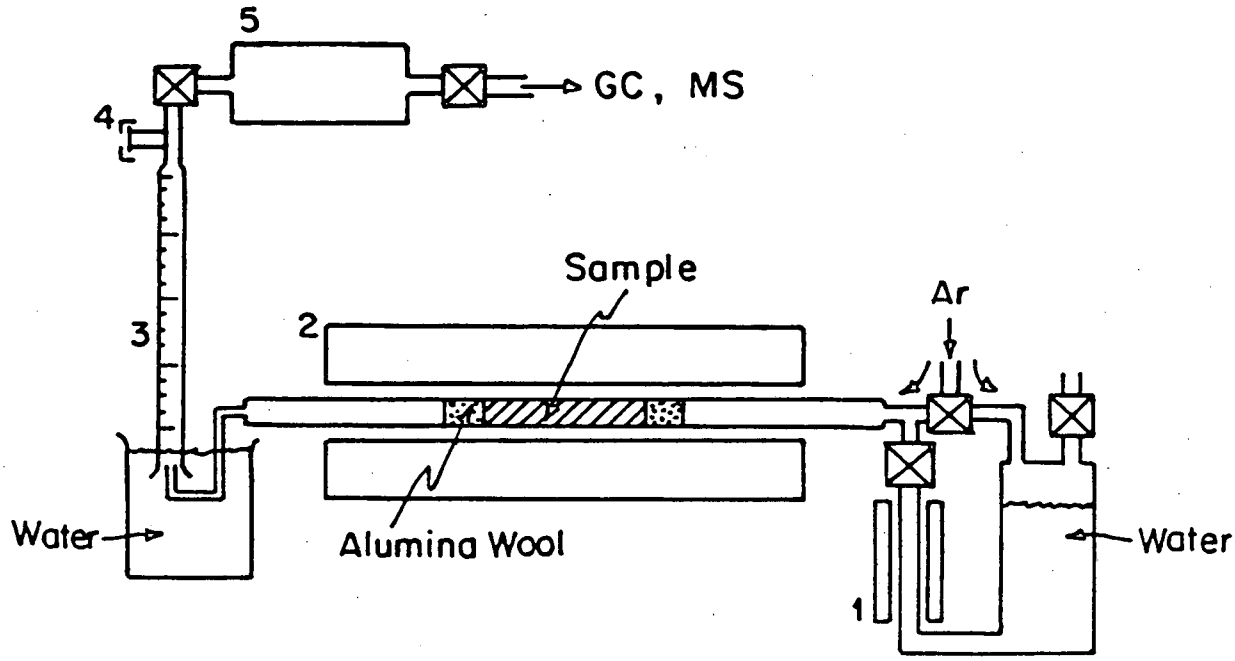

1 Steamer
2 Reactor
3 Burette
4 Septum
5 Vacuum Container

XBL 832-5326

Fig. 1

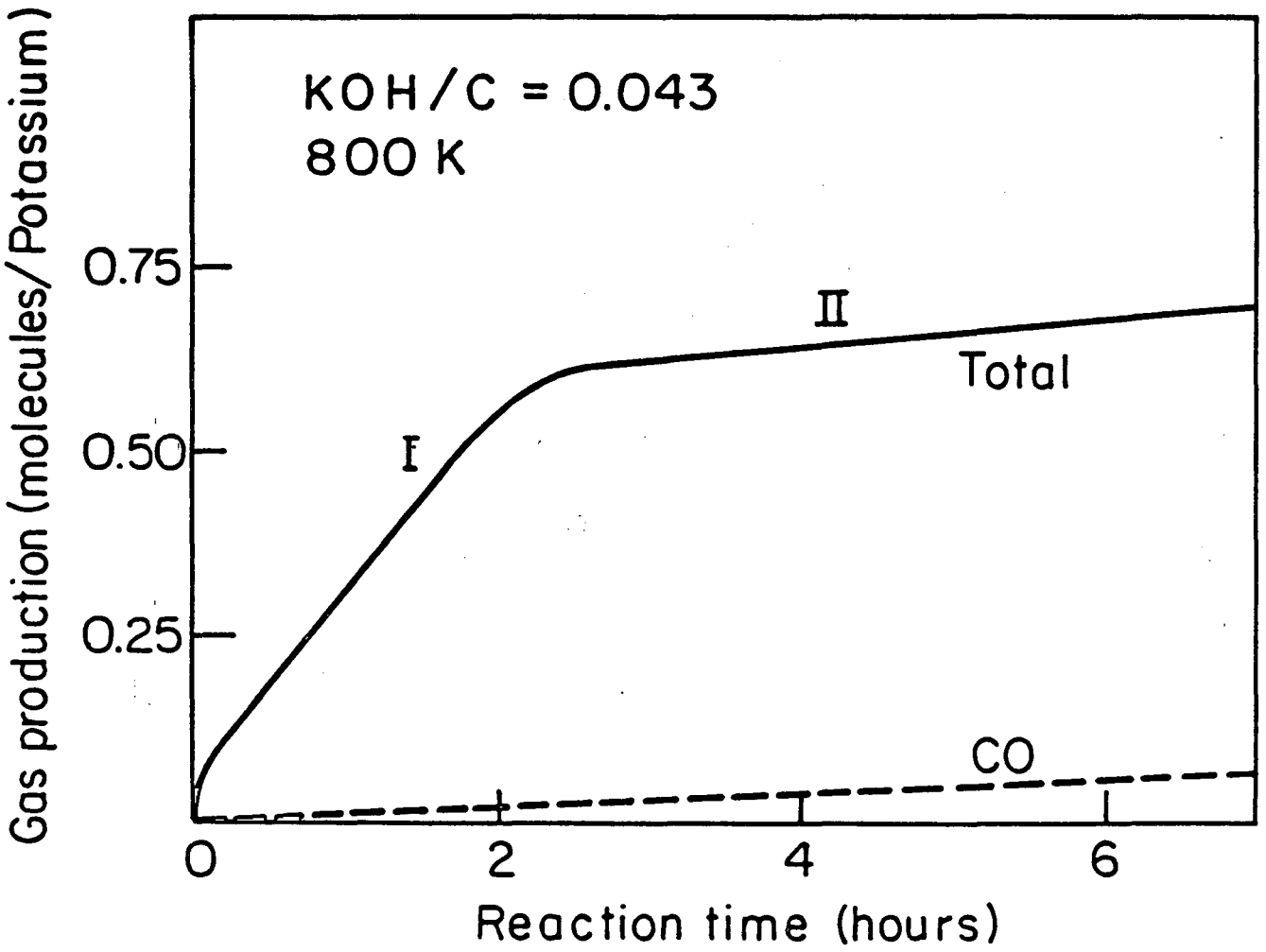

XBL833-8665A

Fig. 2

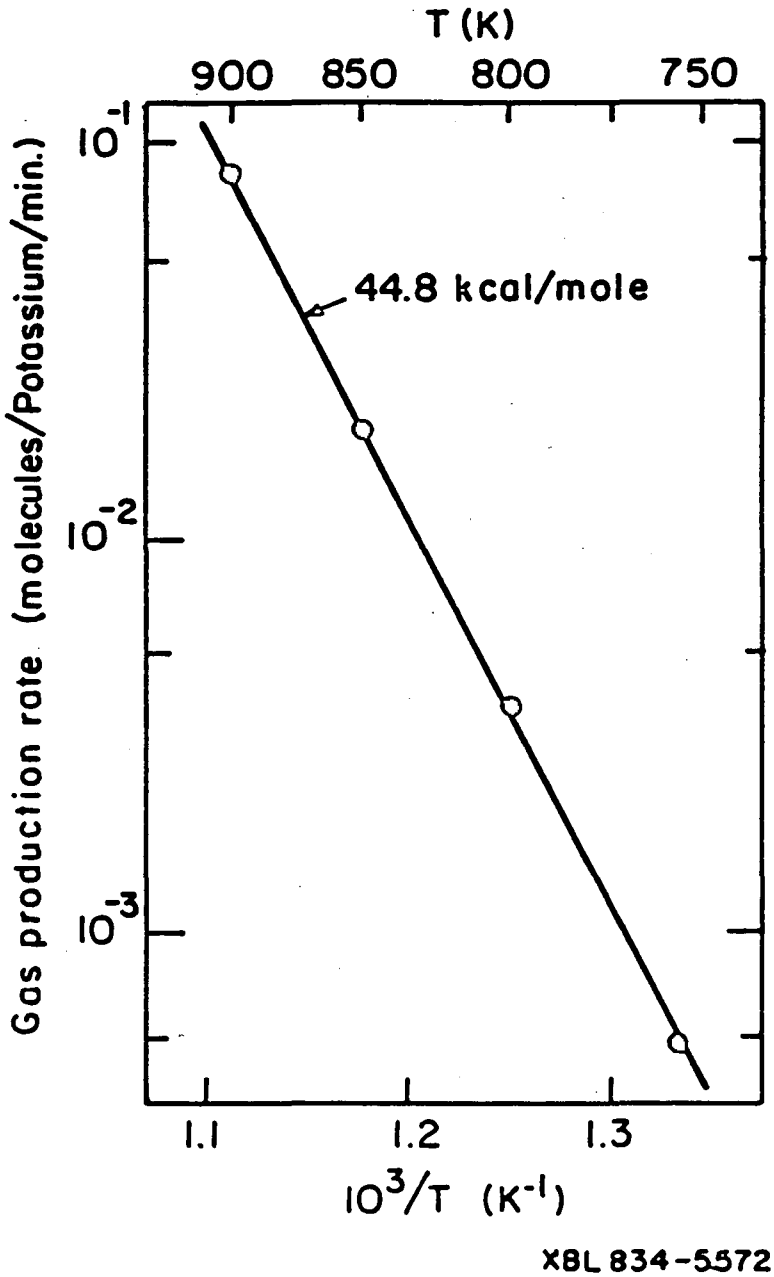
T (K)
900
850
800
750
10^{-1}
10^{-2}
10^{-3}
44.8 kcal/mole
Gas production rate (molecules/Potassium/min.)
1.1
1.2
1.3
$10^3/T$ (K^{-1})
XBL 834-5572

Fig. 3

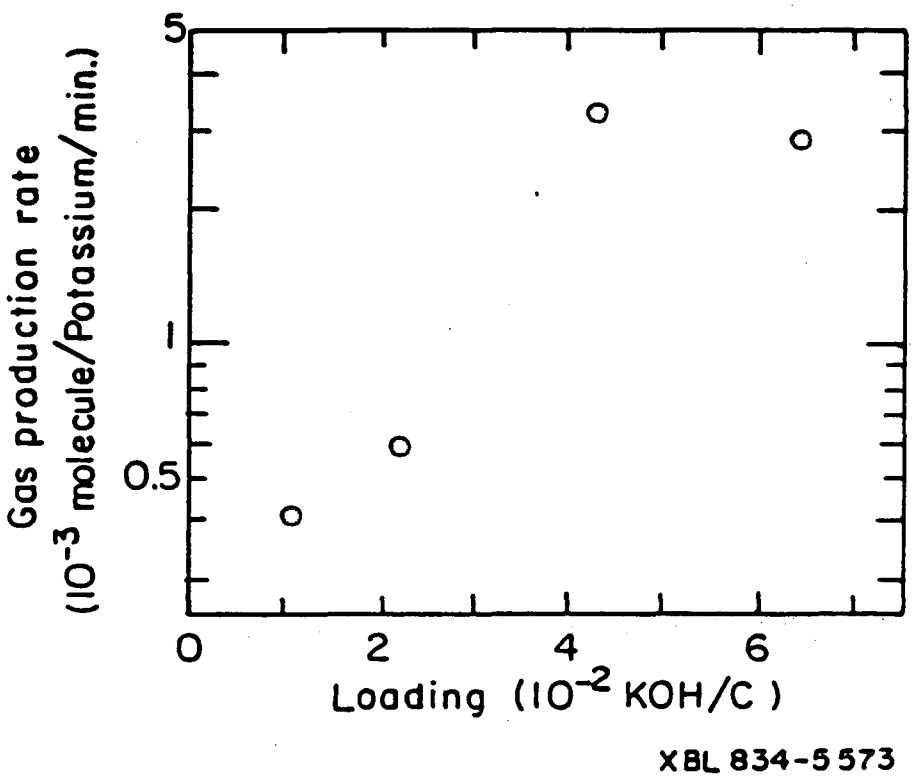
Gas production rate
(10^{-3} molecule/Potassium/min.)
5
1
0.5
0
2
4
6
Loading (10^{-2} KOH/C)
XBL 834-5573

Fig. 4

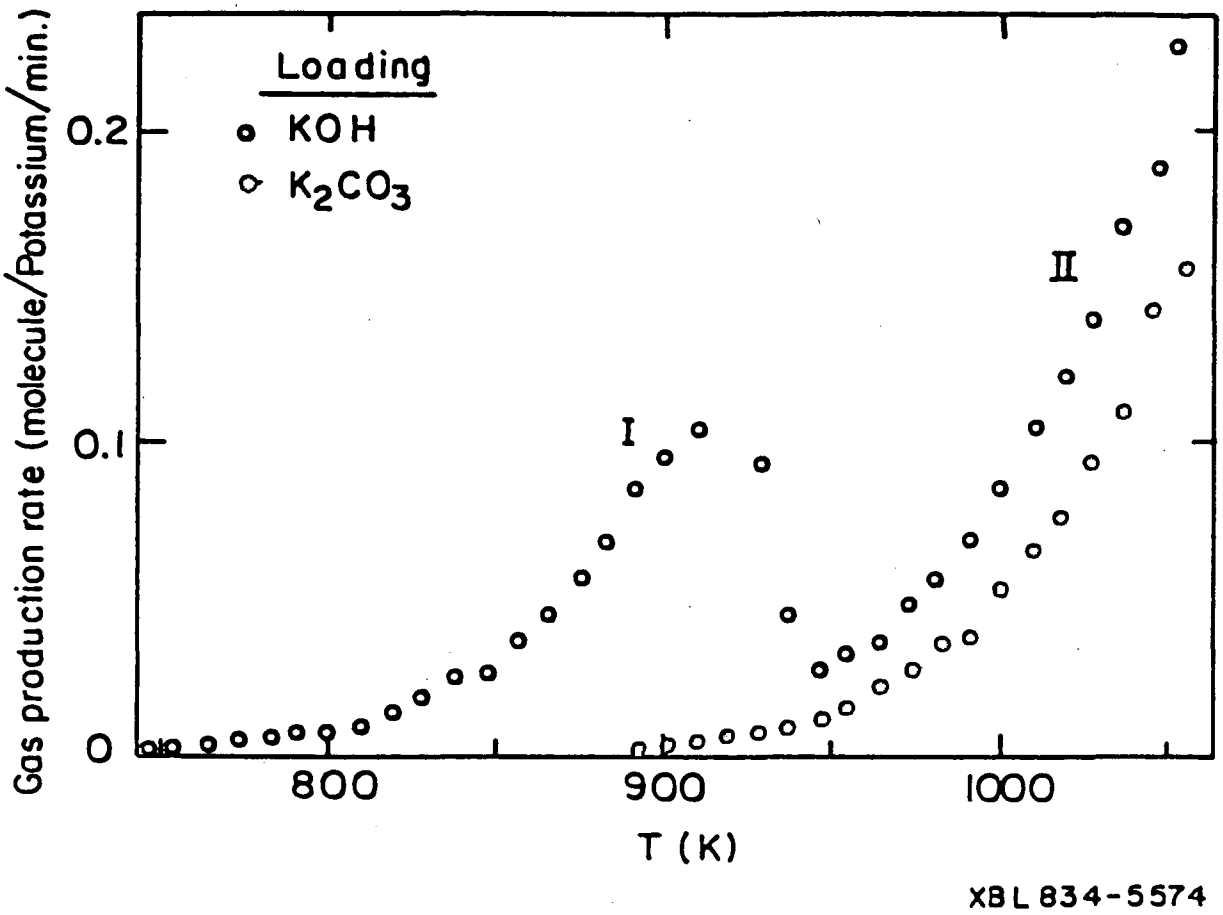
Loading
KOH
K_2CO_3
Gas production rate (molecule/Potassium/min.)
0.2
0.1
0
800
900
1000
T (K)
I
II
XBL 834-5574

Fig. 5

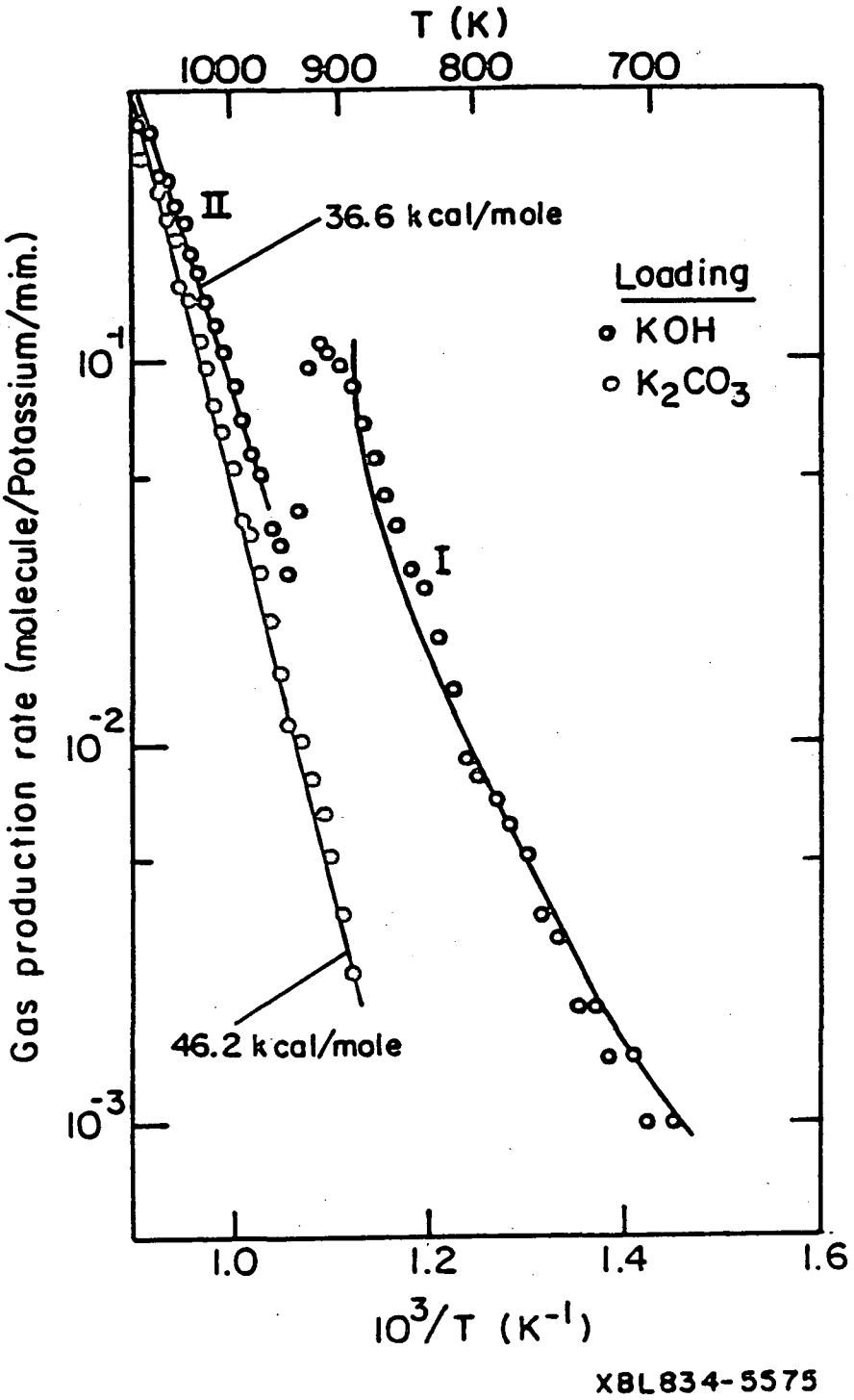
T (K)
1000
900
800
700
II
36.6 kcal/mole
Loading
o KOH
o K_2CO_3
I
46.2 kcal/mole
Gas production rate (molecule/Potassium/min.)
10^{-1}
10^{-2}
10^{-3}
1.0
1.2
1.4
1.6
$10^3/T$ (K^{-1})
XBL834-5575

Fig. 6

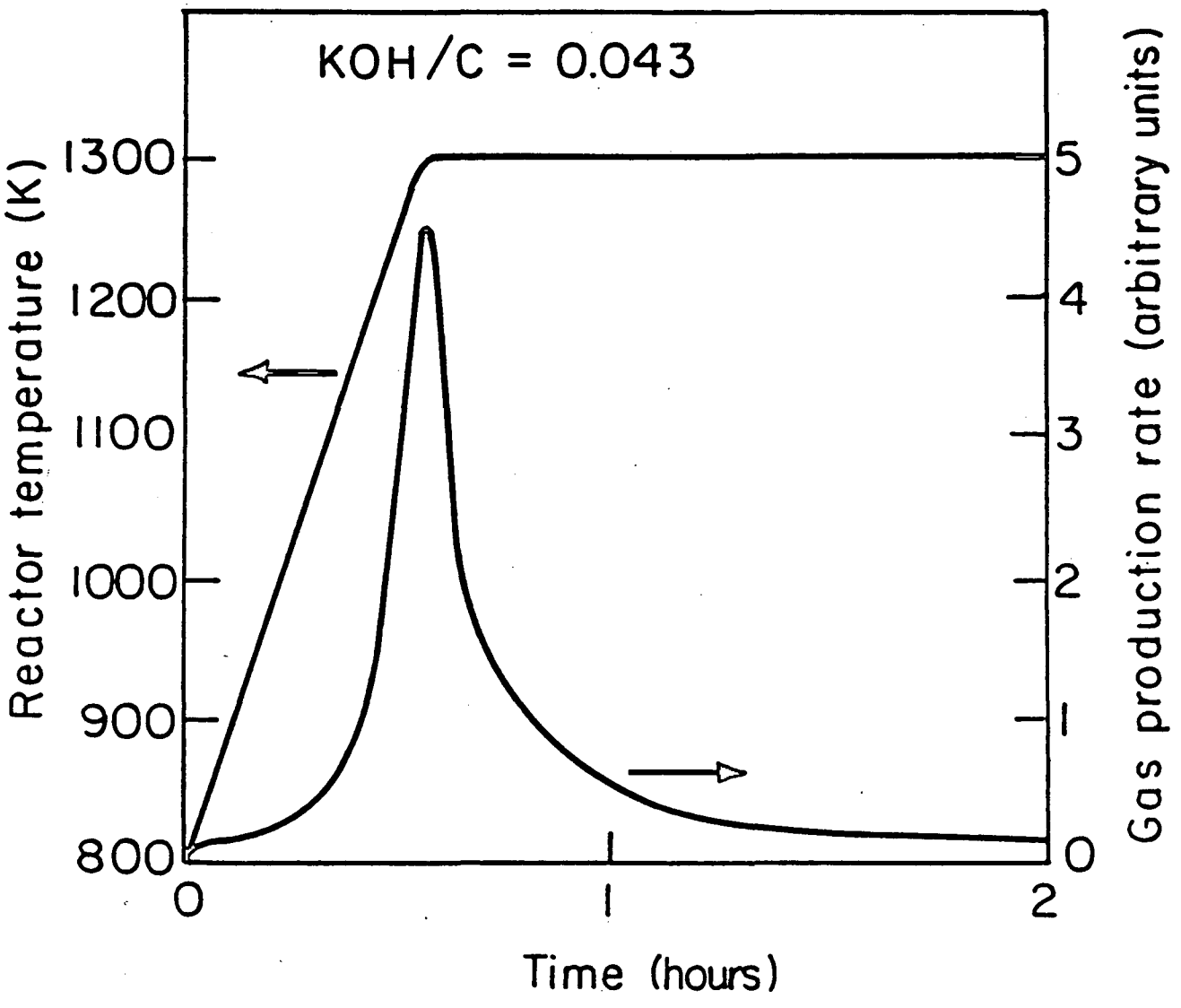
KOH/C = 0.043
Reactor temperature (K)
1300
1200
1100
1000
900
800
Gas production rate (arbitrary units)
5
4
3
2
1
0
0
1
2
Time (hours)
XBL 833-8713A

Fig. 7

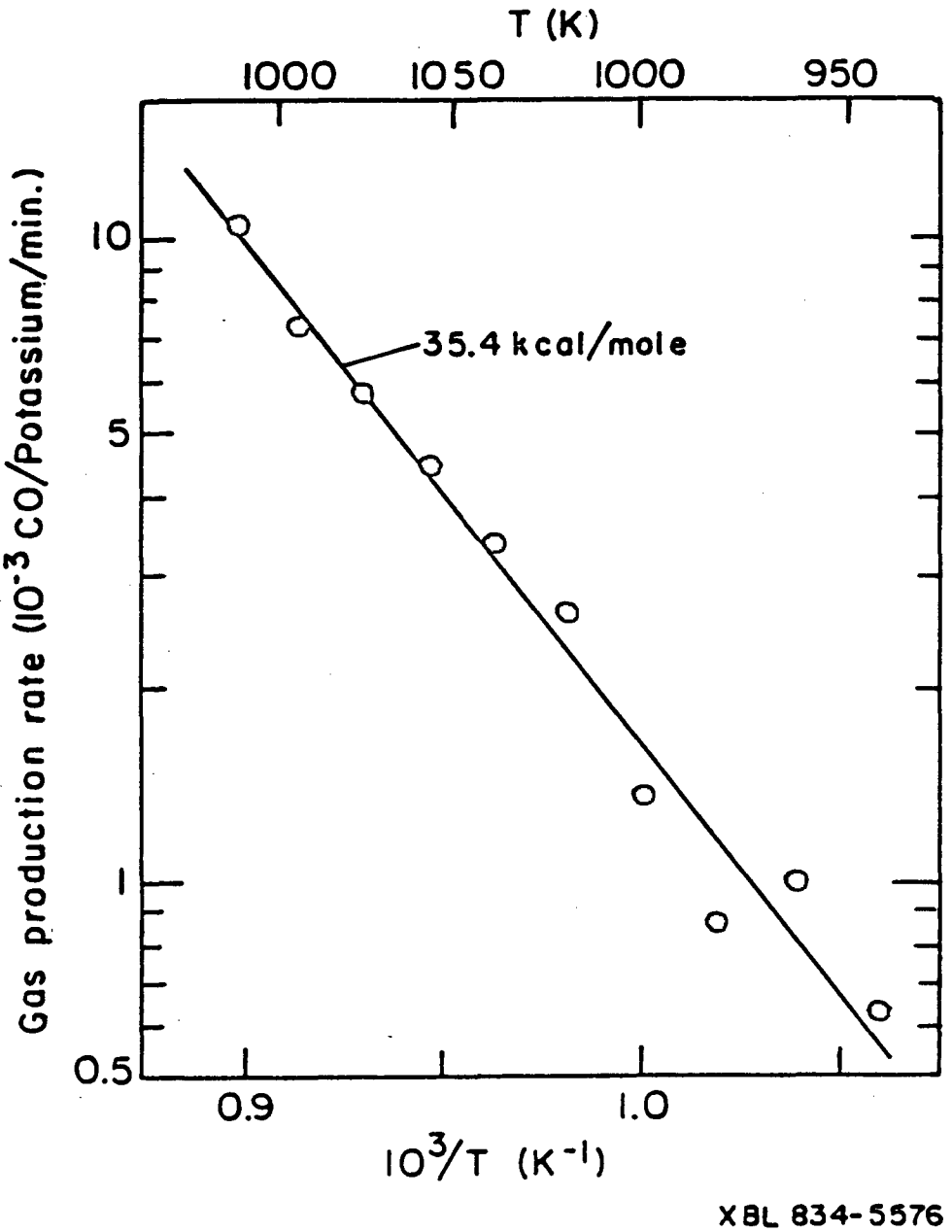
T (K)
1000
1050
1000
950
10
5
1
0.5
Gas production rate (10^{-3} CO/Potassium/min.)
35.4 kcal/mole
0.9
1.0
$10^3/T$ (K^{-1})
XBL 834-5576

Fig. 8

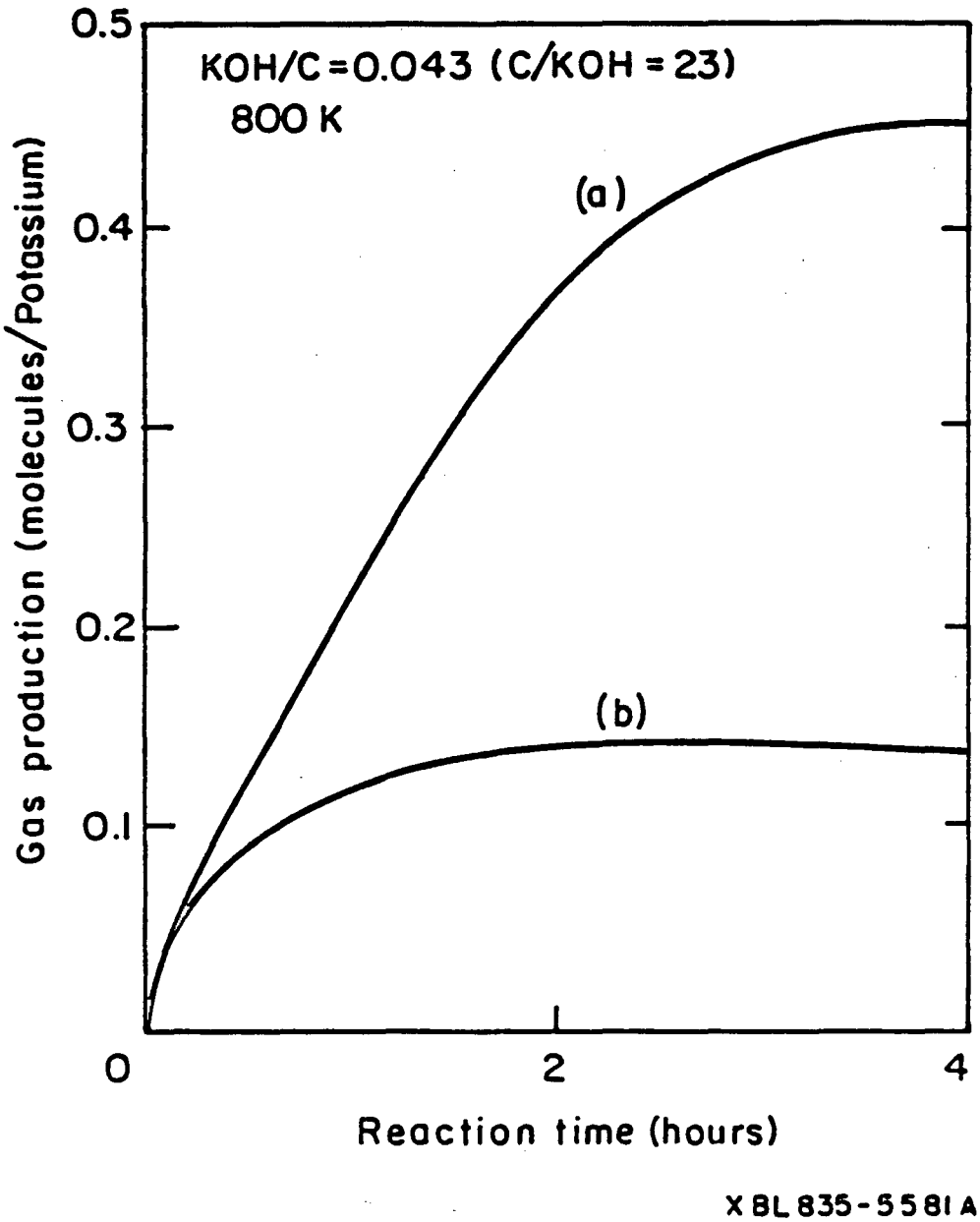
KOH/C=0.043 (C/KOH = 23)
800 K
(a)
(b)
Gas production (molecules/Potassium)
Reaction time (hours)
0.5
0.4
0.3
0.2
0.1
0
2
4
XBL835-5581A

Fig. 9

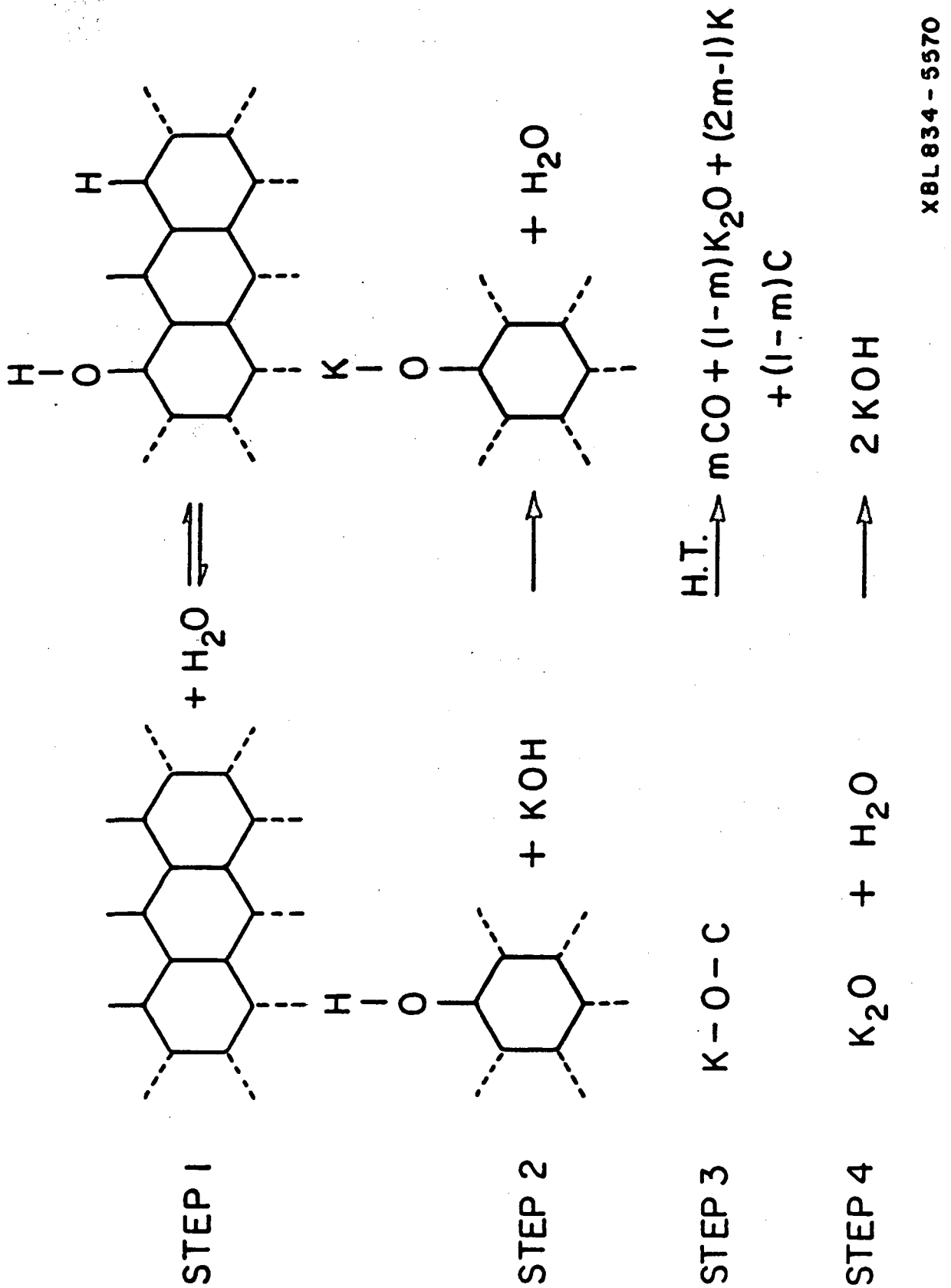
STEP 1
STEP 2
STEP 3
STEP 4
+ H2O
+ KOH
+ H2O
H.T.
mCO + (1-m)K2O + (2m-1)K
+ (1-m)C
2 KOH
K-O-C
K2O + H2O
XBL 834-5570

Fig. 10

LBL-16050

Distribution of Reaction Products in the KOH Initiated Low Temperature Steam Gasification of Graphite

By F. Delannay*, W.T. Tysoe, H. Heinemann and G.A. Somorjai

Materials and Molecular Research Division, Lawrence Berkeley Laboratory
and
Department of Chemistry, University of California, Berkeley, CA 94720

Abstract

Powdered graphite samples loaded with various amounts of KOH have been reacted with atmospheric pressure of steam in the temperature range 700–900K. Significant amounts of C_1 to C_6 hydrocarbons are found in the gaseous products of this reaction. Both the abundance of these hydrocarbons with respect to hydrogen and their relative distribution varies as a function of reaction time, KOH loading and temperature. A model for their production is proposed according to which C–H groups are stabilized by the formation of a potassium phenolate type compound at the prismatic edge of graphite. Hydrocarbon would then be produced from the direct hydrogenation of surface carbon atoms. The hydrocarbon distribution shows large deviations from the ideal Schulz-Flory distribution, giving little support to a chain growth type mechanism.

*On leave from the Groupe de Physico–Chimie Minérale et de Catalyse, Université Catholique de Louvain, Belgium

1. INTRODUCTION

The production of hydrogen and carbon monoxide from the reaction of carbon with water vapor is endothermic and thus requires high temperatures. In contrast, the synthesis of hydrocarbons from carbon monoxide and hydrogen is exothermic and is thus favored at lower temperatures. Our research aims at investigating possible catalytic routes for the direct production of hydrocarbons from the reaction of carbon and steam. As most hydrocarbons are unstable at high temperature, this reaction requires a relatively low reaction temperature.

It has been known for many years that alkali metals catalyse the steam gasification of carbon [e.g. 1]. In most studies reported in the literature, alkalis are deposited over carbon in the form of a salt, usually a carbonate [2]. We have found that, in the temperature range 700-900K, the gasification of graphite powder under atmospheric pressure of steam is more efficiently promoted by potassium hydroxide than by potassium carbonate.[3] The only gaseous products from the reaction are then hydrogen and hydrocarbons. This hydrogen is produced from the splitting of H_2O; the corresponding amount of oxygen remains in the sample to form a compound with potassium. As a consequence, the reaction rate decreases drastically when all potassium hydroxide has been converted into this compound. CO evolves when the latter is decomposed thermally by heating up to 1300K in an inert atmosphere. The original reactivity is partially recovered after this heat treatment. This suggests that the decomposition of this compound consisting of C-OK groups may be the rate limiting step in the catalytic reaction conducted at higher temperatures.

Few studies have been concerned with the product distribution obtained during gasification reactions. Only the evolution of H_2, CO and a few percent of CO_2 and CH_4 has been reported [e.g. 4]. The CH_4 formed is usually thought to arise from the hydrogenation of CO by H_2, this reaction also being catalyzed by potassium carbonate [5]. However, Cabrera et al. [6] have shown that KOH may directly catalyse the production of CH_4 from the reaction of steam with graphite in the temperature range 500-800K. In this case, a reaction of the type

$$2C + 2H_2O \longrightarrow CH_4 + CO_2$$

was postulated.

In this paper, we discuss the distribution of gaseous products collected during the reaction of a KOH loaded graphite powder under atmospheric pressure of steam in the temperature range 700-900K. It will be shown that significant amounts of C_2 to C_6 hydrocarbons are formed in addition to hydrogen and methane. Such a production of higher hydrocarbons has not been reported previously in the literature. Possible reaction mechanisms will be discussed.

2. EXPERIMENTAL

A diagram of the experimental setup is shown in Figure 1. The reactor consisted of an 3.7 mm ID alumina tube containing 0.5 g of KOH loaded graphite powder. Either pure argon or pure steam could be flowed through the reactor. Steam was produced by forcing water from a reservoir

into a copper tube heated to above 400K. At the outlet of the reactor, an open ended U-shaped tube immersed in water condensed the steam and allowed the gaseous products to be collected in a graduated burette. This enabled the volume of gas products to be measured accurately. The volume of cooling water was kept as small as possible to minimize solution of products. However, it should be borne in mind that a variation in solubility of outlet gases may slightly affect the product distribution. A septum was attached to the top of the burette for the extraction of gas samples during the reaction. Gas from the burette was periodically transferred to a vacuum container for analysis after the reaction was completed.

The products were analysed by gas chromatography and mass spectrometry. A thermal conductivity detector with column consisting of six feet Chromosorb 102 + six feet Chromosorb 101 with argon as carrier gas was used for the measurement of the relative proportions of H_2, CO, CO_2 and CH_4. The hydrocarbon distribution was more conveniently determined using flame ionization detection with a six foot long Chromosorb 102 column. This experimental apparatus is discussed in greater detail in reference 3.

3. RESULTS

The experiments discussed in this paper were all performed under isothermal conditions. After exposing the sample to steam at 400K, the reactor temperature was quickly raised (at $\sim$ 160K min^{-1}) to that chosen

for the reaction. Figure 2 shows a plot of the volume of gas produced as a function of time during the reaction at 800K for a sample having a KOH/C molecular ratio of 0.043 (which corresponds to a C/KOH ratio of 24). The shape of this plot is typical for a reaction in the temperature range 700-900K for KOH/C ratios between 0.01 to 0.065 (corresponding to C/KOH ratios of 100 and 16 respectively). After a short initial burst, the gas evolved at a fairly constant rate during a period of a few hours. (This first steady-state will be referred to in the following as reaction I). The reactivity of the sample then changed, and the gas production proceeded at a much reduced rate (reaction II).

During reaction I, the products were almost exclusively hydrogen and hydrocarbons, whereas during reaction II, CO was also produced. In this case the CO/H_2 ratio was approximately unity. Fig. 3 presents a typical flame ionization detection (FID) chromatogram of a gas sample extracted via the septum during the reaction. Hydrocarbons up to C_6 can be detected. Alkenes are more abundant than alkanes. The major C_2 and C_4 peaks on this chromatogram are ethene and butene respectively. (The three C_3 compounds are not separated on this chromatogram. Operation of the GC at lower oven temperature indicated that propene was the dominant C_3 product). No acetylene was detected.

Figure 4 gives the variation of the volume concentration of CH_4 in H_2 for the same reaction illustrated in Figure 2. The amount of CH_4 exceeded 2% of the amount of H_2 during the initial burst. However, the proportion of methane then decreased steeply during reaction I and once again increased slowly during reaction II. The average concentration CH_4 in H_2 in the products after 7 hours was 0.4%.

The corresponding variation of the distribution of the hydrocarbons is shown in Figure 5 as weight % of total hydrocarbon. The proportion of methane ranged between more than 80% at the start and about 50% at the end of reaction I. The proportion of higher hydrocarbons increased progressively during reaction I, with C_4 becoming the most abundant. Little change in the hydrocarbon distribution occurred during reaction II.

Figure 6 and 7 present the variations of the volume concentration of CH_4 in H_2 and the weight distribution of hydrocarbons respectively for the reaction at 800K for a sample having a KOH/C loading equal to 0.01. As discussed in [3], the gas production rate decreased drastically as the loading was decreased. In this case, reaction I lasted about 20 hours. The transition between reactions I and II is gradual. Decreasing the KOH loading by a factor of 4 significantly increased the CH_4/H_2 concentration ratio. This ratio again exhibits a decrease during reaction I. Furthermore, the results displayed in Figure 7 indicate that the proportion of higher hydrocarbons decreased with respect to methane when the KOH loading is decreased. The trends also differ from the previous case (ie. with KOH/C=0.043) as a continuous increase of the proportion of CH_4 with respect to the higher hydrocarbons is now observed. Figure 8 summarizes the dependence of the mean CH_4/H_2 concentration ratio of the products of reaction I on the KOH/C loading of the samples.

The temperature dependence of the product distribution was investigated in the temperature range 700-900K for samples with K/C ratio=0.043. The

experimental points in Figure 9 are for an analysis of gas samples which were extracted via the septum when the amount of hydrogen produced equalled 20% of the potassium loading in each case. The results have been plotted on a semilog scale as a function of the inverse of the absolute temperature. The solid points refer to the volume concentration of CH_4 in H_2, and the open circles ratio to the $(C_2 + C_3)/CH_4$ weight ratio. As the temperature was increased, the proportion of CH_4 was found to decrease both with respect to hydrogen and higher hydrocarbons. The reproducibility of these measurements was not very high, owing probably to the strong dependence of the product distribution on the extent of reaction. No accurate activation energy differences between products may thus be extracted from these data. An order of magnitude estimate may be made, however, and indicates that the activation energy for CH_4 formation is about 5 to 10 kcal/mole lower than for H_2 production.

4. DISCUSSION

Whereas the production of a few percent of methane during steam gasification of carbon is not a new phenomenon, the production of higher hydrocarbons has not been reported before. The high rate observed during reaction I cannot be sustained because of the formation of an oxygen containing (K-O-C) intermediate which is stable at the reaction temperature.[3] However, Figures 5 and 7 indicate that hydrocarbons are produced during both reactions I and II. This supports the suggestion that these two stages of the reaction essentially operate via identical mechanisms, the difference merely being due to a change in the rate controlling step. [3].

According to the model developed [3], under reaction conditions, the prismatic edges of graphite would be covered, as indicated in Figure 10, by K-O-C and H-C groups. The binding within the K-O-C entities may be sufficiently strong to induce C-C bond scission. Hydrogen molecules can desorb as a result of the recombination of two C-H groups.

According to this picture, the simplest mechanism that may be proposed for the production of hydrocarbons would be the formation of multiple $C-H_m$ groups by sequential addition of hydrogen and simultaneous scission of C-C bonds. The formation of such groups on neighboring surface atoms would eventually result in the desorption of hydrocarbon molecules heavier than CH_4. According to this mechanism, the role of potassium would be to effectively increase the number of available hydrogen atoms (by preventing the back-reaction $C-H + C-OH \longrightarrow 2C + H_2O$). Potassium would have little influence on the subsequent formation of the $C-H_m$ groups.

However, our experiments indicate that the product distribution does vary with potassium loading. Although this may merely be due to a dependence of product distribution on gasification rate, this behaviour is somewhat analogous to the role of alkalis in Fischer-Tropsch reactions. Indeed, it is well known that, for example, iron or nickel catalyzed Fischer-Tropsch reactions are influenced by the presence of alkalis in three ways: it (i) decreases the overall rate of hydrogenation, (ii) increases the rate of chain growth and (iii) increases the proportion of alkenes with respect to the alkanes [7.8]. In a similar way, the present results show that increasing the amount of potassium (i) decreases the ratio CH_4/H_2, and

(ii) increases the proportion of higher hydrocarbons with respect to methane. Also, the proportion of alkenes remains fairly high in all cases.

This analogy suggests an alternative possible mechanism for the hydrocarbon formation that would involve, as in Fischer-Tropsch reactions, as shown in [12] the hydrogenation of a carbidic carbon at an active site of the catalyst surface (potassium in the present case) and the subsequent growth of a hydrocarbon chain by sequential addition to the initial $C-H_m$ group of carbon atoms diffusing to this active site. In such a case, the formation of hydrocarbons would be directly catalyzed by potassium.

It is known that potassium has some activity as a catalyst for hydrogenation reactions. It has been reported that, at elevated pressures, a mixture of K_2CO_3 and coal is a good catalyst for the methanation of CO by H_2[5]. Also, Bonzel and Krebs [9] have shown that, after depositing potassium onto an iron foil, Fischer-Tropsh activity was still maintained even though the surface of the catalyst was completely covered by more than ten monolayers of carbon. Auger analysis indicate that, in this case, potassium still lays on top of the carbon deposit.

The distribution of Fischer-Tropsh products can be described by means of a chain growth polymerization mechanism, ie. the so-called Schulz-Flory (SF) distribution [10]. If W_n is the weight fraction of hydrocarbons containing n carbon atoms, this formalism implies that the logarithm of the ratio W_n/n should vary linearly with n. Figure 11 shows such a plot for a typical product

distribution for the reaction of a KOH loaded graphite sample at 800K. The dependence of $\ln(W_n/n)$ on n is obviously not linear. In general, this non-linearity is due either to a larger CH_4 and C_4 yield that expected theoretically or alternatively to a somewhat diminished C_2 and C_3 yield.

However, deviations of Fischer-Tropsch product distribution from the ideal SF model have often been reported in the literature. Various possible reasons for these deviations have been proposed, for example mass transfer limitations, coexistence of different types of active sites, or shape/size selectivity of the support [11]. The fact that the product distributions in this work do not obey the ideal SF dependence on n is thus not a very strong argument for ruling out the existence of a chain growth polymerization mechanism. The first mechanism proposed (namely the direct hydrogenation of the carbon surface) would, however appear more likely.

Previous papers have studied the influence of KOH on the production of CH_4 in the temperature range 500-800K from the reaction of 20 Torr of water vapor with a piece of highly oriented pyrolytic graphite (HOPG, Union Carbide) in a recirculation type reactor [6,12]. The product gas was not analysed for hydrogen and hydrocarbons other than CH_4 in these studies. However, their production using a flow reactor has been reported more recently [13] and the present results are thus in qualitative agreement with these previous ones. Owing to the low water pressure and temperature of these previous measurements, only a few percent of the KOH reacted and hence only the so-called reaction I

was studied since the transition to reaction II would have required excessively long times (several days).

Assuming that all carbon atoms exposed on the geometric surface area of the HOPG sample have an identical activity, a turnover frequency of about $5 \times 10^{-3} CH_4$ molecule per carbon surface atom per second was calculated for the reaction with 20 Torr of water vapor at 800K [12]. The production of methane was also found to be first order with respect to water pressure up to 600 Torr [13]. The rates of CH_4 production measured in the present work (ie. in the flow reactor) are several orders of magnitude lower than the rate that can be calculated by extrapolation from the data of these earlier works. The origin of this discrepancy is unknown. Invoking differences in KOH loadings is obviously not sufficient to justify such a difference in activity. We hope that further work will allow us to clarify this problem.

5. CONCLUSION

This study shows for the first time that hydrocarbons heavier than CH_4 can be directly produced from the reaction of carbon with steam. This production appears to be promoted by the presence of KOH which allows a high rate of gasification at relatively low temperature. Two possible mechanisms for the formation of the hydrocarbon have been discussed: a chain growth polymerization mechanism and a sequential hydrogen addition to the prismatic planes of graphite.

The obvious limitation of this process is the fact that the high rate of gasification induced by KOH is not a catalytic reaction, owing to the

formation of a highly stable oxygen containing intermediate. The present results open however new prospects for a possible alternate route to the production of valuable hydrocarbons from carbonaceous materials. Future work will aim at studying other alkalis and transition metal hydroxides that might play a simlar role to KOH without involving deactivation.

ACKNOWLEDGEMENTS

This work was jointly supported by the Director, Office of Energy Research, Office of Basic Energy Sciences, Chemical Sciences Division, and the Assistant Secretary for Fossil Energy, Office of Coal Research, Liquefaction Division of the U.S. Department of Energy under Contract Number DE-AC03-76SF00098 through the Pittsburgh Energy Technology Center, Pittsburgh, Pa. We also acknowledge partial support of this research by the Air Products Corporation.

The authors are indebted to G.T. Yee for experimental assistance. F.D. acknowledges Fulbright and NATO research fellowships.

REFERENCES

1. H.S. Taylor and H.A. Neville, J. Am. Chem. Soc., 43, 2065 (1921).
2. D.W. McKee, Carbon, 20, 59 (1982).
3. F. Delannay, W.T. Tysoe, H. Heinemann and G.A. Somorjai, submitted to Carbon.
4. M.J. Veraa and A.T. Bell, Fuel, 57, 194 (1978).
5. N.C. Nahas, Fuel, 62, 239 (1983).

6. A.L. Cabrera, H. Heinemann and G.A. Somorjai, J. Catalysis, 75, 7-22 (1982).

7. R.B. Anderson, in "Catalysis, Vol 4" (P.H. Emmett ed.), Reinhold, New York, 1956.

8. H.H. Storch, N. Golumbic and R.B. Anderson, The Fischer-Tropsch and Related Syntheses, Wiley, New York, 1951.

9. H.P. Bonzel and H.J. Krebs, Surface Science, 109, L527 (1981).

10. G. Henrici-Olive and S. Olive, Angew. Chem., 88, 144 (1976).

11. P.A. Jacobs and D. Van Wouwe, J. Molecular Catalysis, 17, 145 (1982).

12. R. Casanova, A.L. Cabrera, H. Heinemann and G.A. Somorjai, Fuel, in press.

13. F. Delannay, W.T. Tysoe, H. Heinemann and G.A. Somorjai, Proceedings of the 1983 Intern. Conf. on Coal Science, in press.

FIGURE LEGENDS

Figure 1: Diagram of experimental apparatus.

Figure 2: Plot of the gas production as a function of reaction time at 800K for a KOH/C loading equal to 0.043 (KOH/C molecular ratio).

Figure 3: Typical gas chromatogram for hydrocarbon products.

Figure 4: Plot of dependence on reaction time of the CH_4 concentration in H_2 the gas products for a KOH/C loading equal to 0.043 (mol).

Figure 5: Plot of dependence on reaction time of the proportion (wt %) of hydrocarbons for a KOH/C loading equal to 0.043 (mol).

Figure 6: Plot of dependence on reaction time of the CH_4 concentration in H_2 the products for a KOH/C loading equal to 0.01 (mol)

Figure 7: Plot of dependence on reaction time of the wt % proportion of hydrocarbons for a KOH/C loading equal to 0.01 (mol)

Figure 8: Plot of dependence of the CH_4 concentration in H^2 in the products on the KOH/C loading.

Figure 9: Semilog plot of the $(C_2+C_3)/CH_4$ weight ratio (0) and CH_4/H_2 volume ratio (•) as a function of the inverse of the absolute

temperature of the reaction.

Figure 10: Schematic diagram of the various species present on the prismatic edges of graphite during reaction.

Figure 11: Schulz-Flory plot of a typical hydrocarbon distribution in the products. n is the number of carbon atoms in the molecule and W_n is the total weight percent of the C_n hydrocarbons.

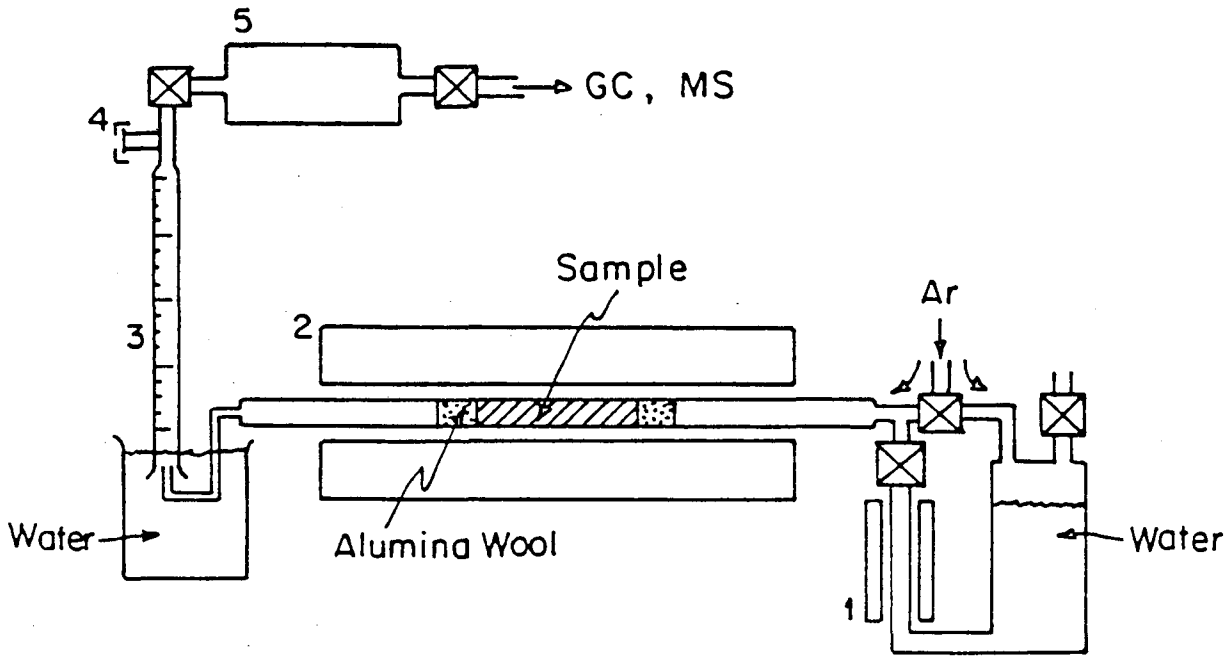

1 Steamer
2 Reactor
3 Burette
4 Septum
5 Vacuum Container

XBL 832-5326

Fig. 1

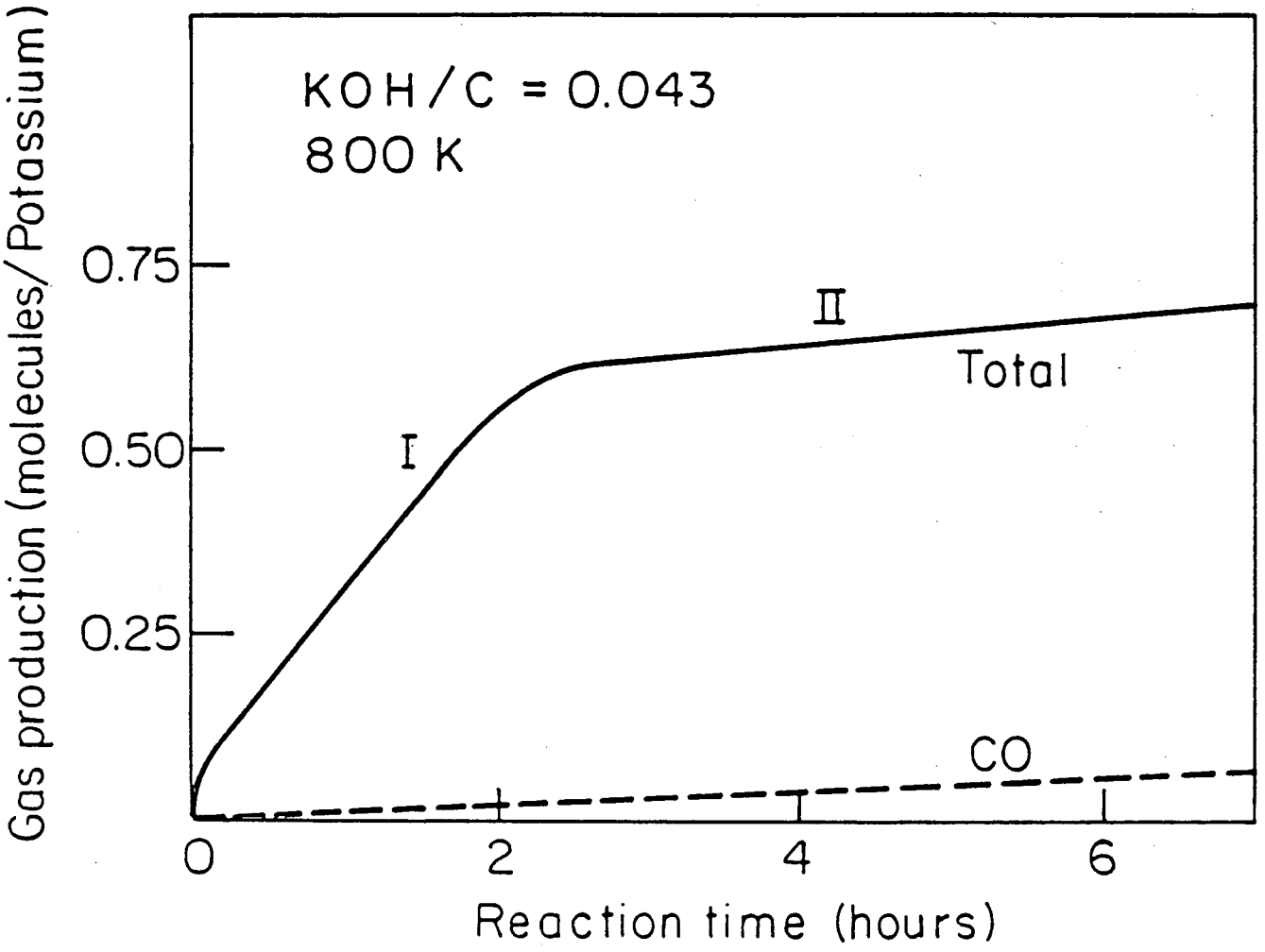
KOH/C = 0.043
800 K
0.75
0.50
0.25
I
II
Total
CO
0
2
4
6
Gas production (molecules/Potassium)
Reaction time (hours)
XBL 833-8665 A

Fig. 2

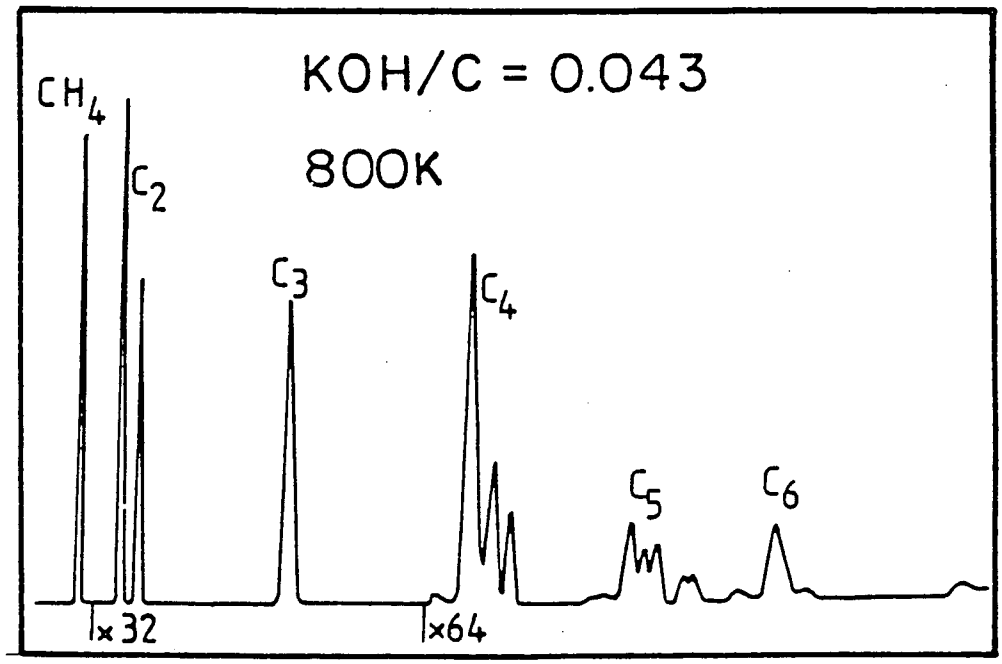

-- XBL 833-8664 A --

Fig. 3

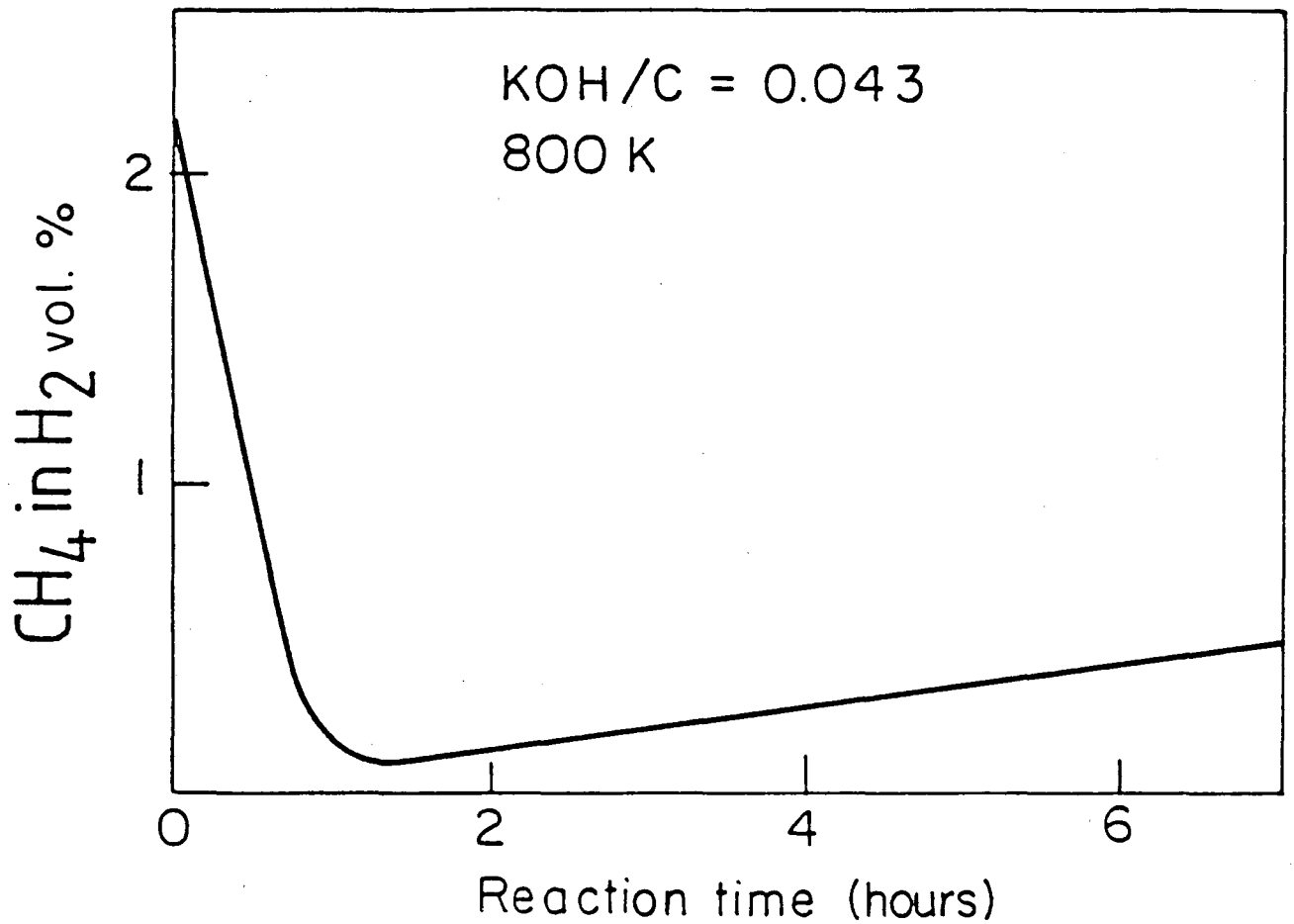

XBL 833-8663A

Fig. 4

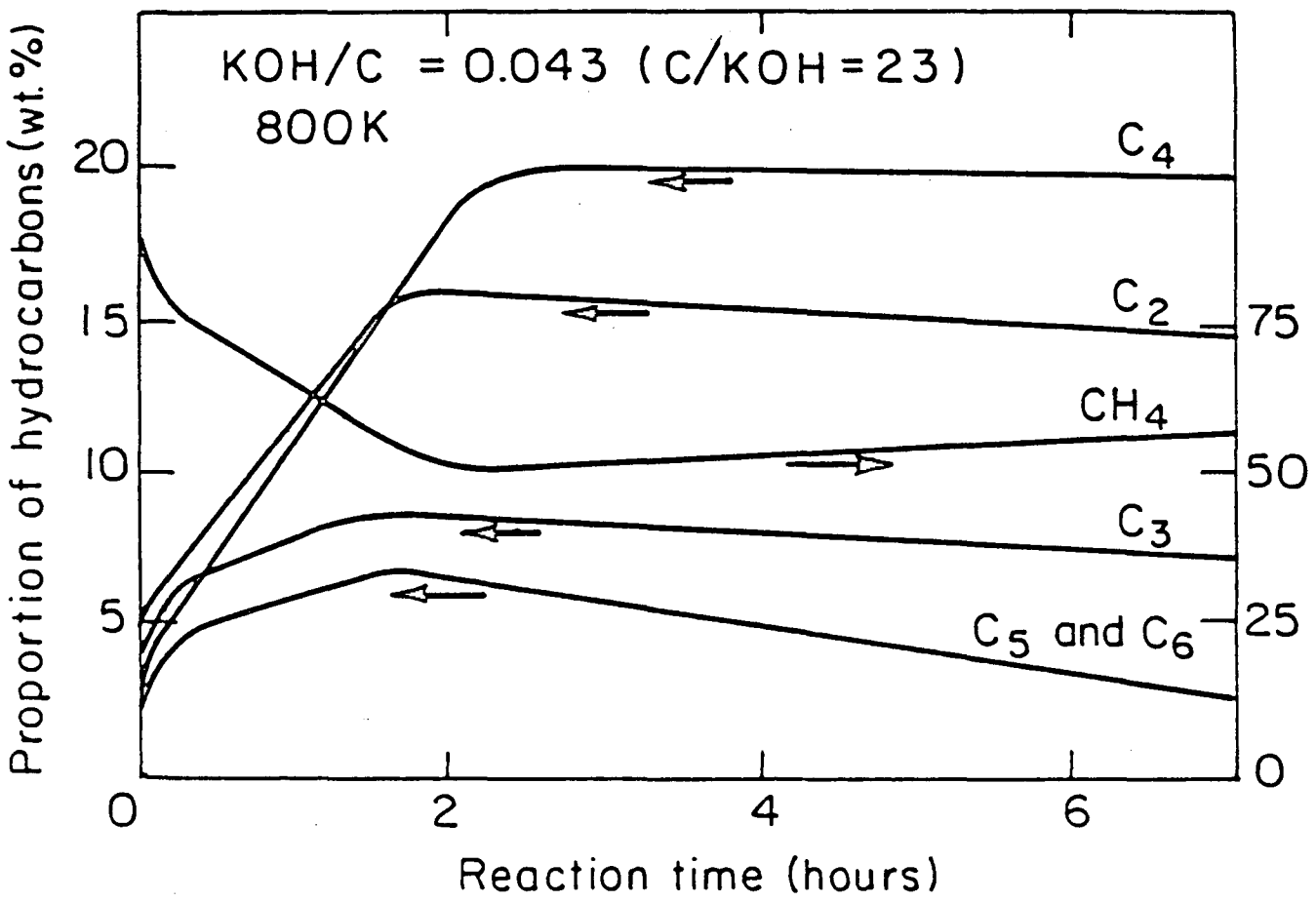
KOH/C = 0.043 (C/KOH = 23)
800K
C4
C2
CH4
C3
C5 and C6
Proportion of hydrocarbons (wt.%)
Reaction time (hours)
0
2
4
6
5
10
15
20
25
50
75
XBL833-8659B

Fig. 5

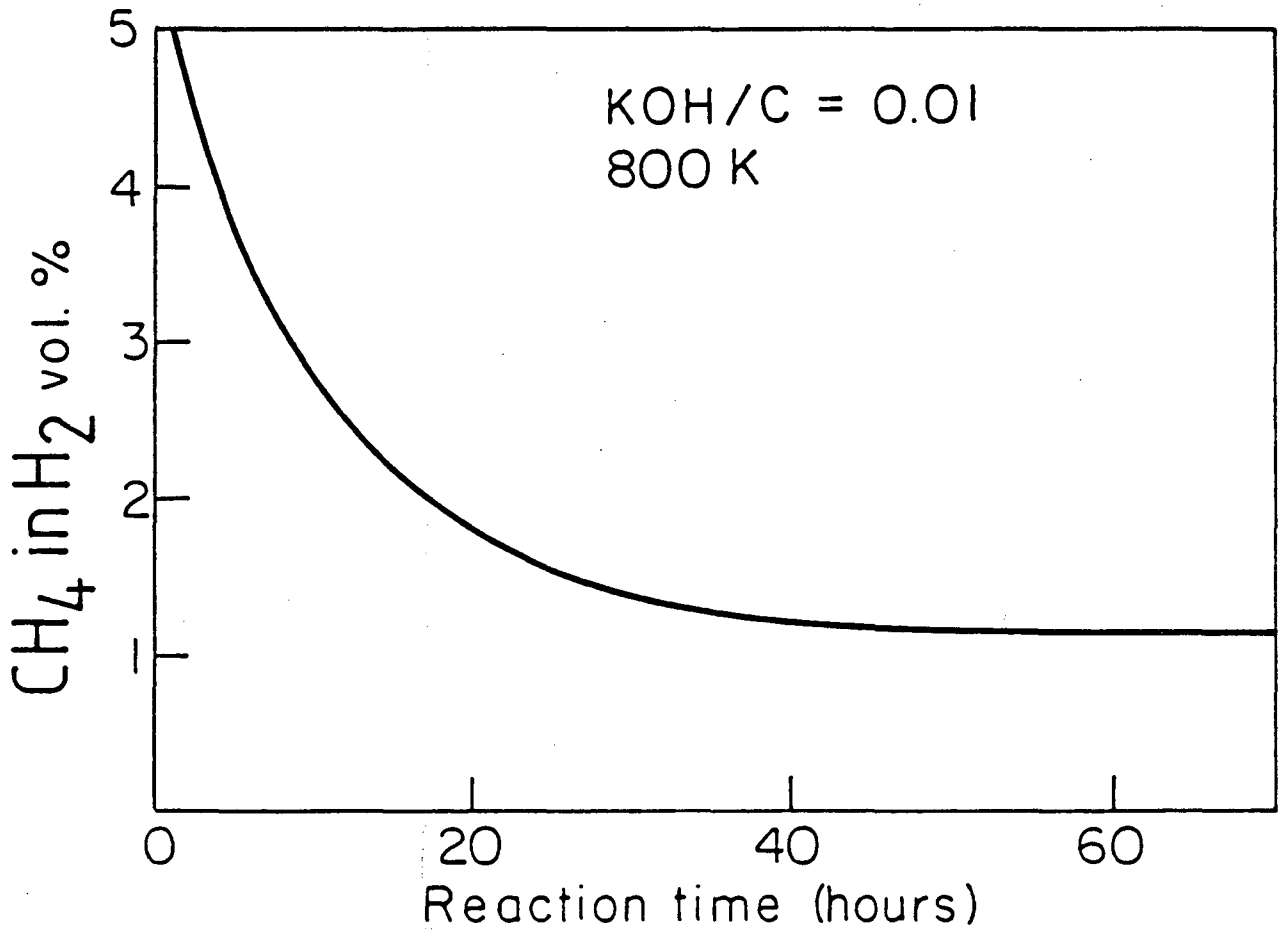
KOH/C = 0.01
800 K
CH_4 in H_2 vol. %
5
4
3
2
1
0
20
40
60
Reaction time (hours)
XBL833-8661A

Fig. 6

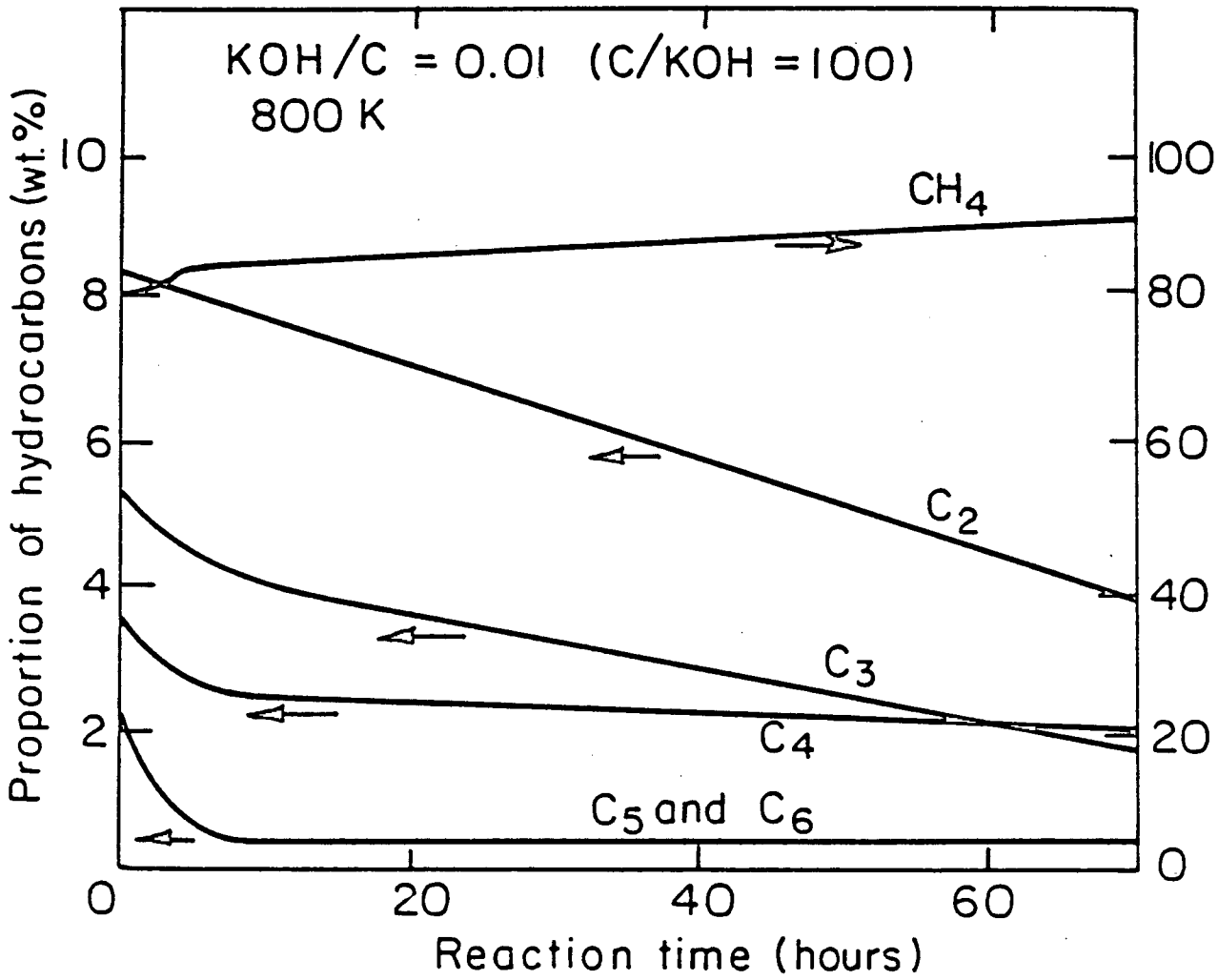
KOH/C = 0.01 (C/KOH = 100)
800 K
Proportion of hydrocarbons (wt.%)
10
8
6
4
2
0
100
80
60
40
20
0
CH_4
C_2
C_3
C_4
C_5 and C_6
0
20
40
60
Reaction time (hours)
XBL833-8660B

Fig. 7

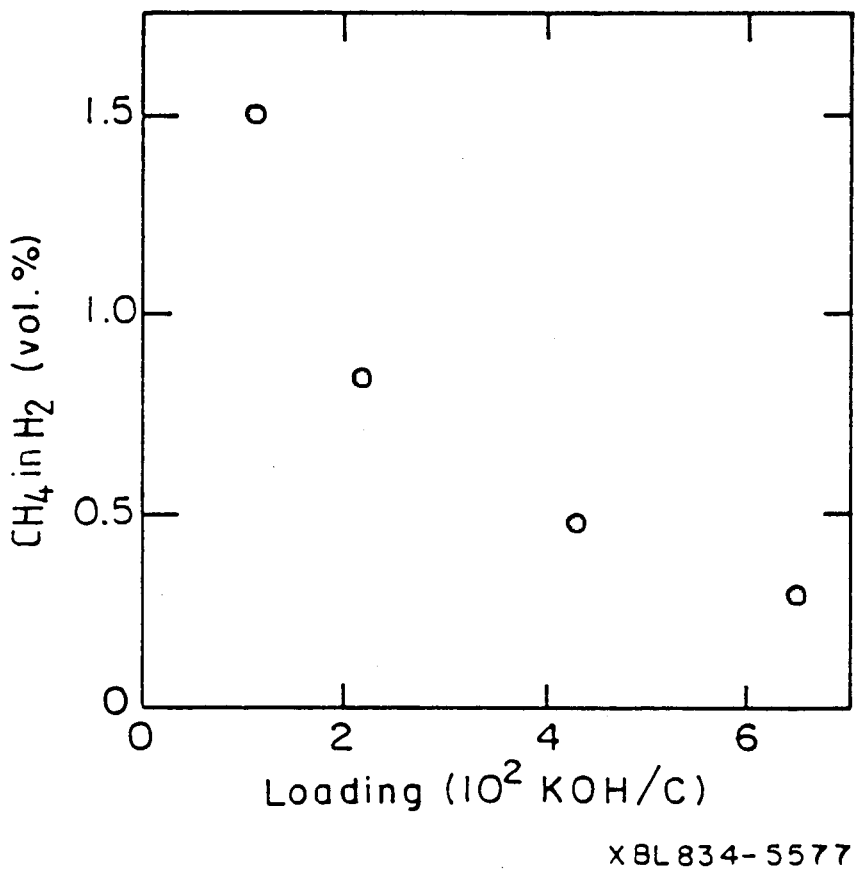

Fig. 8

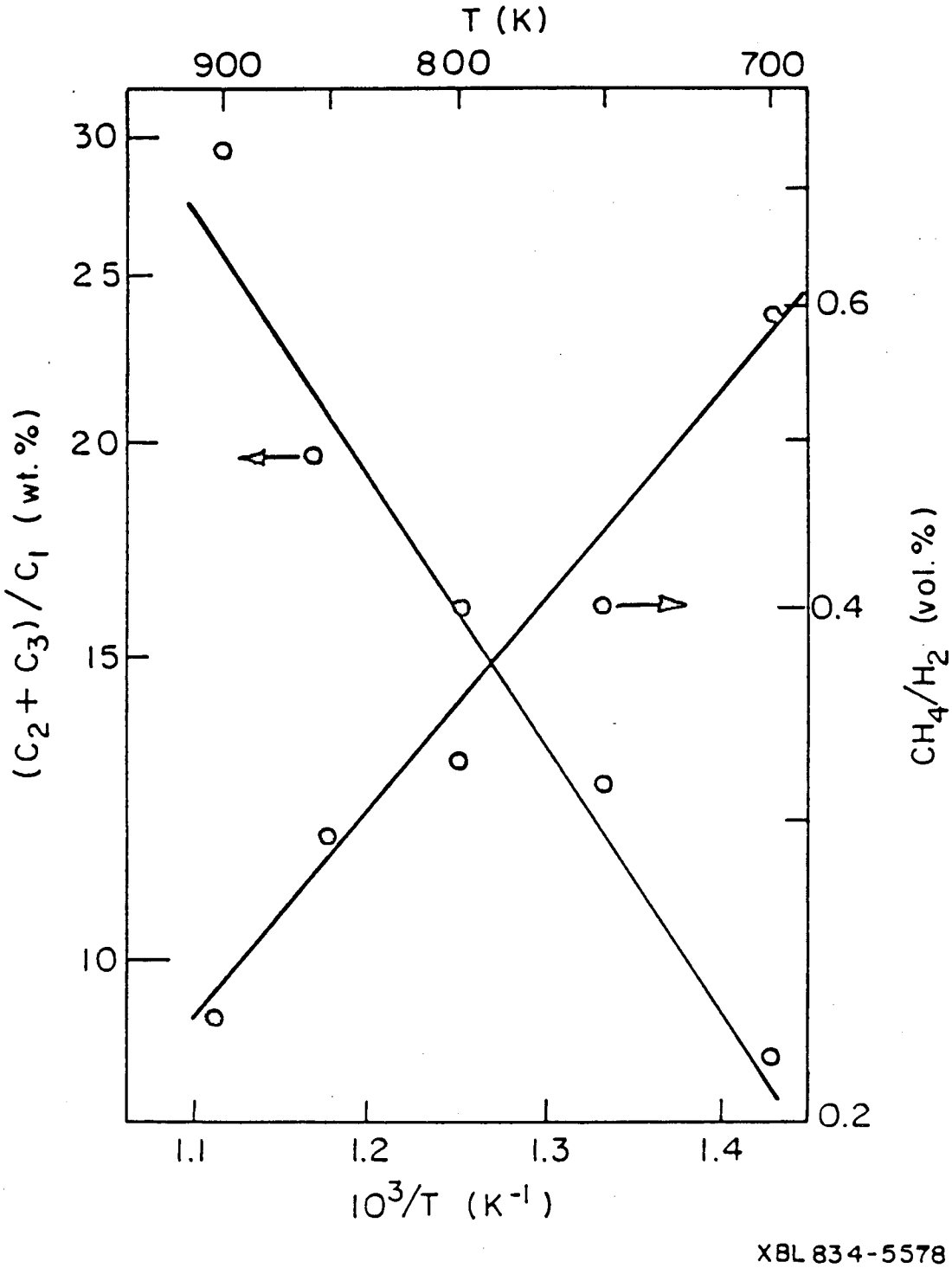
T (K)
900
800
700
30
25
20
15
10
0.6
0.4
0.2
1.1
1.2
1.3
1.4
$(C_2 + C_3)/C_1$ (wt.%)
CH_4/H_2 (vol.%)
$10^3/T$ (K^{-1})
XBL 834-5578

Fig. 9

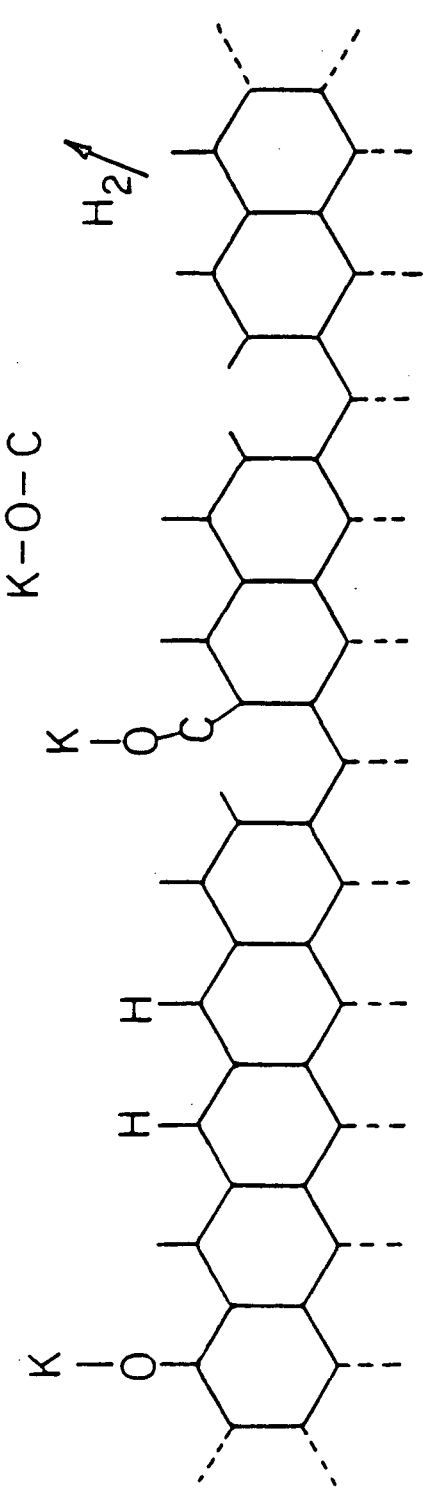

XBL834-5571

Fig. 10

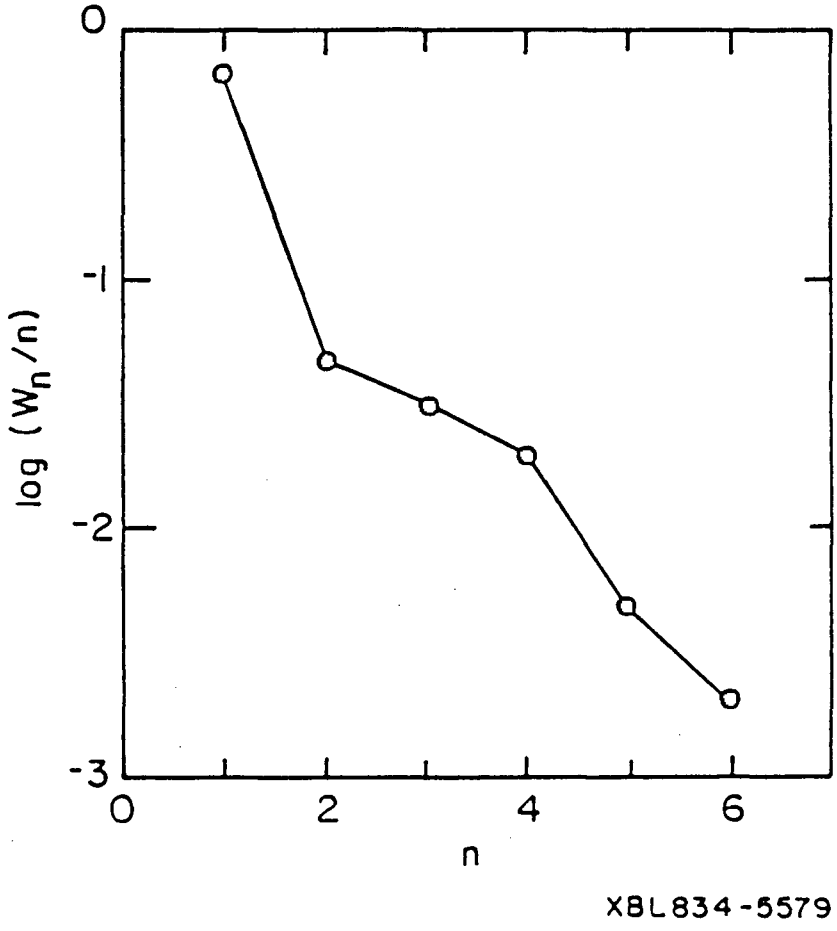

Fig. 11

TECHNICAL INFORMATION DEPARTMENT
LAWRENCE BERKELEY LABORATORY
UNIVERSITY OF CALIFORNIA
BERKELEY, CALIFORNIA 94720